Measurement of Ionizing Radiation

Lecture notes from the third-year undergraduate course *Merjenje ionizirajočega sevanja* (Measurement of Ionizing Radiation) given by prof. dr. Boštjan Golob at the Faculty of Mathematics and Physics at the University of Ljubljana in the academic year 2020-21. Credit for the material covered in these notes is due to professor Golob, while the voice, typesetting, and translation to English in this document are my own.

Disclaimer: This document will inevitably contain some mistakes—both simple typos and legitimate errors. Keep in mind that these are the notes of an undergraduate student in the process of learning the material himself, so take what you read with a grain of salt. If you find mistakes and feel like telling me, I will be grateful and happy to hear from you, even for the most trivial of errors. You can reach me by email, in English, Slovene, or Spanish, at ejmastnak@gmail.com.

For more notes like this, visit ejmastnak.com/fmf

Elijan J. Mastnak
Summer semester 2020-21
Last update: October 10, 2022
Faculty of Mathematics and Physics, University of Ljubljana

Contents

1 Interaction of Particles with Matter

1.1 Charged Particles in Matter

We begin our course with heavy charged particles. For our purposes, a particle is "heavy" if its mass exceeds the electron mass by multiple orders of magnitude, i.e. $m_{\text{particle}} \gg m_{\text{e}}$. Protons, alpha particles, and ions are all examples of heavy particles. This chapter rests on the following obvious but important property:

> Heavy ionizing particles loose energy and change direction as they travel through matter.

Both processes—energy loss and change of direction—are stochastic, and result from, in order of importance,

- Inelastic collisions of ionizing particles with electrons within the material. This is the dominating process contributing to energy loss of ionizing particles as they travel through matter, and is significant because matter contains many more electrons than nuclei.
- Elastic collisions with nuclei within the material.
- Cherenkov radiation.
- Bremsstrahlung processes (for electrons) and nuclear reactions (relevant for heavy particles).

In the remainder of this chapter we will analyze how charged particles loose energy and change direction as they travel through matter.

1.1.1 Semi-Classical Analysis of Ionizing Energy Losses

- We begin with a semi-classical analysis of a heavy charged particle's ionizing energy losses in matter. Our assumptions are:
  1. The electrons in the material with which the ionizing particle interacts are approximately free.
  2. The electric field between ionizing particle and electrons is approximately constant during the interaction. Equivalently, the electrons move only slightly during the interaction with the ionizing particle, and the interaction is short.
  3. The ionizing particle does not change direction significantly when interacting with electrons, which follows from the heavy mass assumption $m \gg m_{\text{e}}$.
- Consider an ionizing particle of mass m and charge $q = ze_0$ moving along the x axis through matter at speed v. This ionizing particle interacts with electrons in the material via the electromagnetic interaction; we begin by analyzing the particle's interaction with electrons within a cylindrical shell of radius $[b, b + \mathrm{d}b]$ centered on the x axis. We assume an electrostatic Coulomb interaction of the form $F = qE$, and relate the *electron*'s change in momentum Δp_{e} to the force's impulse by

$$\Delta p_{\text{e}} = \int F \,\mathrm{d}t = e_0 \int E_\perp \,\mathrm{d}t,$$

  where the time integral runs over the (short) interaction time between the electron and ionizing particle. We take only the electric field component $E_\perp$ perpendicular to

the x axis, because any contributions from the longitudinal component are equal in magnitude and opposite in direction on either side of the electron, and cancel out as the ionizing particle flies past along the x axis. To be clear, E is the electric field caused by the ionizing particle and felt by the electron (and *not* the electron's electric field).

- Next, we change integration variables from time to position according to

$$\Delta p_\mathrm{e} = e_0 \int E_\perp \,\mathrm{d}t = e_0 \int E_\perp \frac{\mathrm{d}x}{v} = \frac{e_0}{v} \int E_\perp \,\mathrm{d}x, \tag{1.1}$$

where we have moved the charged particle's velocity v, which we approximate as constant over the course of the particle-electron interaction, outside the integral. We find the electric field $E_\perp$ with Gauss's law, using a cylinder of radius b centered on the x axis. Gauss's law reads

$$\oiint \mathbf{E} \cdot \mathrm{d}\mathbf{S} = \frac{q}{\epsilon_0} \implies \int E_\perp \cdot (2\pi b \,\mathrm{d}x) = \frac{z e_0}{\epsilon_0},$$

where $q = z e_0$ is the ionizing particle's charge. We rearrange to get

$$\int E_\perp \,\mathrm{d}x = \frac{z e_0}{2\pi \epsilon_0 b},$$

which we then combine with the Equation 1.1 to get

$$\Delta p_\mathrm{e} = \frac{e_0}{v} \int E_\perp \,\mathrm{d}x = \frac{z e_0^2}{2\pi \epsilon_0 v b}.$$

In our semi-classical model, using the just-derived change in momentum, the electron gains corresponding energy equal to

$$\Delta E(b) = \frac{\Delta p_\mathrm{e}^2}{2 m_\mathrm{e}} = \frac{z^2 e_0^4}{8\pi^2 \epsilon_0^2 m_\mathrm{e} v^2 b^2}. \tag{1.2}$$

This result is the energy gained by one electron—or alternatively the energy lost by an ionizing particle—in an interaction between the ionizing particle and a single electron a radial distance b from the x axis.

- We now generalize the single-electron energy loss in Equation 1.2 to many electrons. Let n_e be the number density of electrons in matter; then the total energy lost by the ionizing particle due to electrons in the region $\mathrm{d}V$ between b and $b + \mathrm{d}b$ is

$$\mathrm{d}E(b) = -\Delta E(b) \cdot n_\mathrm{e} \,\mathrm{d}V = -\Delta E(b) \cdot n_\mathrm{e} \cdot (2\pi b \,\mathrm{d}b \,\mathrm{d}x).$$

This expression is the energy *lost* by the ionizing particle, while Equation 1.2 is energy *gained* by an electron, which explains the minus sign. After substituting in ΔE from Equation 1.2 and "dividing" by $\mathrm{d}x$, we have

$$-\frac{\mathrm{d}E(b)}{\mathrm{d}x} = \frac{z^2 e_0^4 n_\mathrm{e}}{8\pi^2 \epsilon_0^2 m_\mathrm{e} v^2 b^2} (2\pi b \,\mathrm{d}b) = \frac{z^2 e_0^4 n_\mathrm{e}}{4\pi \epsilon_0^2 m_\mathrm{e} v^2} \frac{\mathrm{d}b}{b}, \tag{1.3}$$

which is the energy E lost by ionizing particle per distance x traveled along x axis due to electrons between b and $b + \mathrm{d}b$.

- To get total energy losses, we integrate Equation 1.3 over all relevant values of b—for now we write this simply as $b \in [b_{\min}, b_{\max}]$ and get

$$-\frac{\mathrm{d}E}{\mathrm{d}x} = \frac{z^2 e_0^4 n_\mathrm{e}}{4\pi\epsilon_0^2 m_\mathrm{e} v^2} \ln \frac{b_{\max}}{b_{\min}}. \tag{1.4}$$

  We will find the appropriate values of $b_{\min}$ and $b_{\max}$ from our assumption of a short-range ionizing interaction, which rules out electrons farther than some to-be-determined distance $b_{\max}$.

Finding $b_{\min}$

- To find $b_{\min}$, we begin with Equation 1.2, which we write in the form

$$\Delta E \propto \frac{1}{b^2}.$$

  The takeaway here is that, because of the reciprocal relationship between E and b, maximum energy loss and minimum distance are related by

$$\Delta E_{\max} \propto \frac{1}{b_{\min}^2}.$$

  Our plan is to find maximum energy loss, then invert the relationship for $b_{\min}$.

- Maximum energy loss occurs for a head-on collision of electron and ionizing particle. Assuming the ionizing particle and electrons' speeds after the collision are v' and v_e, respectively, then conservation of energy and momentum give

$$mv = mv' + m_\mathrm{e} v_\mathrm{e} \qquad \text{and} \qquad mv^2 = m(v')^2 + m_\mathrm{e} v_\mathrm{e}^2,$$

  which we can solve for final electron velocity to get

$$v_\mathrm{e} = \frac{2v}{1 + \frac{m_\mathrm{e}}{m}} \approx 2v.$$

  For the sake of completeness, we derive this by solving for v' in the momentum conservation, substituting this into the energy equation, and rearranging to get

$$\underbrace{v' = v - \frac{m_\mathrm{e}}{m} v_\mathrm{e}}_{\text{from momentum}} \implies \underbrace{2 m_\mathrm{e} v v_\mathrm{e} = \frac{m_\mathrm{e}^2}{m} v_\mathrm{e}^2 + m_\mathrm{e} v_\mathrm{e}^2}_{\text{from energy}}.$$

  We then divide through by $m_\mathrm{e} v_\mathrm{e}$ and solve for v_e to get

$$v_\mathrm{e} = \frac{2Mv}{m_\mathrm{e} + M} = \frac{2v}{1 + \frac{m_\mathrm{e}}{M}} \approx 2v.$$

- In any case, using $v_\mathrm{e} \approx 2v$, the hypothetical maximum energy gained by the electron from a head-on collision with an ionizing particle is

$$\Delta E_{\max} = \frac{1}{2} m_\mathrm{e} (2v)^2.$$

  We then substitute this maximum single-electron energy loss into Equation 1.2 to get

$$\Delta E_{\max}(b_{\min}) = \frac{1}{2} m_\mathrm{e} (2v)^2 = \frac{z^2 e_0^4}{8\pi^2 \epsilon_0^2 m_\mathrm{e} v^2} \frac{1}{b_{\min}^2}.$$

We then approximately account for relativistic energy corrections by writing $v \to \gamma v$, where γ is the ionizing particle's gamma factor $\gamma = \left(1 - \frac{v^2}{c^2}\right)^{-1/2}$. This gives

$$\frac{1}{2} m_\mathrm{e} (2\gamma v)^2 = \frac{Z^2 e_0^4}{8\pi^2 \epsilon_0^2 m_\mathrm{e} v^2} \frac{1}{b_\mathrm{min}^2} \implies b_\mathrm{min} = \frac{Z e_0^2}{4\pi\epsilon_0 \gamma m_\mathrm{e} v^2},$$

which is our final expression for the minimum interaction distance b_min between electrons and the ionizing particle.

Finding b_max

- We find b_max using the assumption of a short duration interaction, which means that the electron does not move significantly over the course of the interaction. We know formalize the meaning of "short interaction time". We first assume electrons are bound to their nuclei with an average binding energy

$$\langle W_\mathrm{b} \rangle = h\nu,$$

where the frequency ν determines the energy scale of the nucleus-electron interaction, and sets a corresponding characteristic nucleus-electron interaction time

$$\tau = \frac{1}{\nu}.$$

Meanwhile, the interaction time between the electron and the ionizing particle is of the order $t \sim b/v$, so our condition for short ionizing particle-electron interaction is

$$t < \tau = \frac{1}{\nu}.$$

- Once again, we include a semi-classical relativistic correction, this time accounting for time dilation, which we write $t \to t/\gamma$. This correction produces

$$\frac{t}{\gamma} < \tau = \frac{1}{\nu} \implies \frac{b}{\gamma v} < \frac{1}{\nu} \implies b < \frac{\gamma v}{\nu},$$

where we have substituted in $t \sim b/v$. An estimate for the maximum interaction distance b_max between an ionizing particle and electrons is then

$$b_\mathrm{max} \sim \frac{\gamma v}{\nu} = \frac{\gamma h v}{\langle W_\mathrm{b} \rangle}.$$

Result

- We now substitute the expressions for b_min and b_max into the expression for ionizing losses in Equation 1.4, which produces

$$-\frac{\mathrm{d}E}{\mathrm{d}x} = \frac{n_\mathrm{e} z^2 e_0^4}{4\pi\epsilon_0^2 m_\mathrm{e} v^2} \ln\left(\frac{4\pi\gamma^2 v^2 \epsilon_0 m_\mathrm{e} h}{z e_0^2 \langle W_\mathrm{b} \rangle}\right). \tag{1.5}$$

It remains to find an estimate for electron number density n_e. We find this from

$$n_\mathrm{e} = Z n_\mathrm{at} = Z\rho \frac{N_\mathrm{A}}{M_\mathrm{m}},$$

where Z is the atomic number of the material through which the ionizing particle travels (used to get the number of electrons per atom), n_at is the number density of atomic nuclei in the material, ρ is the material's mass density, M_m is the material's molar mass, and N_A is Avogadro's number.

- Finally, we introduce the classical electron radius r_e, which sets a length scale for problems involving electrons and electromagnetic interactions; the classical electron radius is defined from the relationship

$$m_\mathrm{e}c^2 = \frac{e_0^2}{4\pi\epsilon_0 r_\mathrm{e}},$$

which equates the relativistic mass energy $m_\mathrm{e}c^2$ to the electrostatic energy at the radius r_e. In terms of the fine structure constant $\alpha = \frac{1}{4\pi\epsilon_0}\frac{e_0^2}{\hbar c}$, the classical radius is

$$r_\mathrm{e} = \frac{e_0^2}{4\pi\epsilon_0 m_\mathrm{e}c^2} = \frac{\alpha\hbar c}{m_\mathrm{e}c^2}.$$

- In terms of the electron number density n_e and classical radius r_e, the expression for ionizing energy losses in Equation 1.5 becomes

$$-\frac{\mathrm{d}E}{\mathrm{d}x} = \frac{r_\mathrm{e}}{\epsilon_0}\underbrace{\frac{z^2e_0^2}{\beta^2}}_{\text{particle}}\underbrace{Z\rho\frac{N_\mathrm{A}}{M_\mathrm{m}}}_{\text{material}}\ln\left(\frac{\gamma^2\beta^3ch}{zr_\mathrm{e}\langle W_\mathrm{b}\rangle}\right). \tag{1.6}$$

The first set of constants depends on the ionizing particle's properties and the second set on the material's properties: z is the ionizing particle's charge in units of e_0 and Z is the material's atomic number.

- Finally, without derivation, a more thorough analysis of ionizing losses performed with quantum mechanical considerations, including corrections for electron spin, leads to the *Bethe formula*

$$-\frac{\mathrm{d}E}{\mathrm{d}x} = \frac{4\pi}{m_\mathrm{e}c^2}\cdot\frac{n_\mathrm{e}z^2}{\beta^2}\cdot\left(\frac{e_0^2}{4\pi\epsilon_0}\right)^2\left[\ln\left(\frac{2m_\mathrm{e}c^2\gamma^2\beta^2}{I}\right)-\beta^2\right]. \tag{1.7}$$

The quantity I is called the *mean excitation potential*; this is an energetic quantity of the order 10 or 100 eV and roughly describes the energy needed to excite an atom in the ionized material.

Interpretation

- For easier interpretation, we first re-write the ionizing energy losses (Eq. 1.6) as

$$-\frac{\mathrm{d}E}{\mathrm{d}x} = \frac{a}{\beta^2}\ln\left(b\gamma^2\beta^3\right), \tag{1.8}$$

where we have defined

$$a = \frac{Z^2e_0^2n_\mathrm{e}}{\epsilon_0}Z_\mathrm{a}\rho_\mathrm{a}\frac{N_\mathrm{A}}{M_\mathrm{a}} \qquad \text{and} \qquad b = \frac{ch}{Zr_\mathrm{e}\langle W_\mathrm{b}\rangle}.$$

Our goal is to analyze energy loss as a function of particle speed. First, we note that the $\frac{1}{\beta^2}$ term in Equation 1.8 dominates at small β, while the logarithm term dominates at large β. The expression for $\frac{\mathrm{d}E}{\mathrm{d}x}$ diverges at $\beta \to 0$ and reaches a maximum as $\beta \to 1$. There is a minimum in between for $\beta \in (0, 1)$.

- In principle, to find the minimum we would find the derivative of $\frac{\mathrm{d}E}{\mathrm{d}x}$ with respect to β, set this equal to zero, and find the solution $\beta_{\min}$. We won't do this here and simply quote the result: a transcendental equation of the form

$$\ln\left[b\gamma^2\beta^3\right] = \frac{3}{2} + \frac{\beta^2}{1-\beta^2},$$

where we note that γ depends on β. Again without proof, the minimum turns out to be largely independent of b, and for most particles occurs in the range

$$\beta_{\min} \approx 0.96,$$

quite near the speed of light. Charged particles moving through matter at a speed $\beta_{\min}$ for which Equation 1.8 is minimized (i.e. the speed corresponding to minimum possible ionizing losses) are called *minimum ionizing particles*, or MIPs.

1.1.2 Ionizing Losses in Momentum and Position Space

- We now consider the dependence of an ionizing particle's losses $\frac{\mathrm{d}E}{\mathrm{d}x}$ on the particle's momentum cp. Minimum ionizing losses occur at roughly the same β for all particles. At any fixed value of β, particles with smaller m will have smaller cp, so particles with low mass have minimum energy losses at smaller values of pc than heavy particles.
- Finally, we consider the dependence of a ionizing particle's losses on the particle's distance x traveled through matter—we will assume the particle comes to a full stop, and does not pass through the material.

  Roughly sketched: $-\frac{\mathrm{d}E}{\mathrm{d}x}$ is small at small values of x, when a particle just entered a material, and initially increase rapidly with increasing distance traveled through the material (as the particle slows and deposits energy). Ionizing losses culminate in a large peak just before the end of the particle's path, and then of course plummets to $-\frac{\mathrm{d}E}{\mathrm{d}x} = 0$ when the particle stops (the particle can't deposit energy after it stops moving).

  Note that Equation 1.8 predicts a particle's losses $-\frac{\mathrm{d}E}{\mathrm{d}x}$ increase indefinitely with decreasing particle speed β. This contradicts reality, in which a particle eventually stops; the discrepancy occurs because of the many approximations involved in deriving Equation 1.8.

1.1.3 Range of an Ionizing Particle in Matter

- Because ionizing losses are a stochastic process, not every particle will have the same range when traveling through matter—some will travel further before stopping and some shorter.
- Consider the probability $P(x)$ that an ionizing particles reaches a distance x into material before stopping. Hypothetically, if every particle had the exact same range, say R, then this plot would be a step function of the form

$$P(x) = \begin{cases} 1 & x \leq R \\ 0 & x > R. \end{cases}$$

In other words, all would particles reach precisely the range $x = R$ and no particle makes it further. This does not occur in practice, since particle range is a random

variable dependent on stochastic processes. In practice, $P(x)$ is a probability distribution spread out about a central value, e.g. R_0. Conventionally, range for ionizing radiation is defined as the position reached by 50 percent of incident particles.

Range of an Low-Speed Ionizing Particle

- In this section, we will show that the range of a low-speed ionizing particle in matter is proportional to the square of the particle's kinetic energy T, i.e.

$$R \propto T^2.$$

To show this, we first relate range R to the above expression for ionizing losses $\frac{\mathrm{d}E}{\mathrm{d}x}$ as follows. For an incident ionizing particle with mass m and kinetic energy T, range is the distance traveled before the particle comes to a halt, where $T = 0$ and $E = mc^2$. We express the dependence of range on incident kinetic energy with the integral

$$R(T) = \int_{T+mc^2}^{mc^2} \frac{\mathrm{d}x}{\mathrm{d}E}\,\mathrm{d}E = \int_T^0 \frac{\mathrm{d}x}{\mathrm{d}E}\,\mathrm{d}T,$$

where $E = mc^2 + T$ is the particle's total relativistic energy. We then invert the integrand and switch the limits of integration to get

$$R(T) = -\int_0^T \left(\frac{\mathrm{d}E}{\mathrm{d}x}\right)^{-1} \mathrm{d}T. \tag{1.9}$$

- Next, we make the auxiliary calculation

$$T = E - mc^2 = \gamma mc^2 - mc^2 = (\gamma - 1)mc^2, \tag{1.10}$$

followed by a small-β Taylor approximation of $\gamma - 1$, which reads

$$\gamma - 1 = \frac{1 - \sqrt{1-\beta^2}}{\sqrt{1-\beta^2}} \approx \left[1 - \left(1 - \tfrac{\beta^2}{2}\right)\right] \cdot \left(1 + \tfrac{\beta^2}{2}\right) \approx \frac{\beta^2}{2}.$$

We then substitute $\gamma - 1 \approx \beta^2/2$ into Equation 1.10 to get

$$T = (\gamma - 1)mc^2 \approx \frac{mc^2}{2} \cdot \beta^2.$$

The key takeaway for us here is the proportionality $T \propto \beta^2$ for $\beta \ll 1$.

- Next, we recall from Equation 1.8 that for $\beta \ll 1$, a particle's energy losses obey

$$-\frac{\mathrm{d}E}{\mathrm{d}x} \propto \frac{1}{\beta^2}.$$

We then substitute in the small β proportionality $T \propto \beta^2$ and rearrange to get

$$-\frac{\mathrm{d}E}{\mathrm{d}x} \propto \frac{1}{\beta^2} \approx \frac{1}{T} \implies -\left(\frac{\mathrm{d}E}{\mathrm{d}x}\right)^{-1} \propto T.$$

Finally, we substitute this estimate for $\left(\frac{\mathrm{d}E}{\mathrm{d}x}\right)^{-1}$ into Equation 1.9 for range to get

$$R(T) = -\int_0^T \left(\frac{\mathrm{d}E}{\mathrm{d}x}\right)^{-1} \mathrm{d}T \propto \int_0^T T\,\mathrm{d}T = \frac{1}{2}T^2.$$

Lesson: the range of a non-relativistic (i.e. $\beta \ll 1$) particle is proportional to the square of its initial kinetic energy.

1.1.4 Interaction of Matter with Relativistic Particles

- In this section, we will study the behavior of relativistic ionizing particles in matter, and come to the (probably intuitive) conclusion that as the speed of an ionizing particle increases, the particle interacts with more and more particles in the matter through which it travels.

- Consider an ionizing particle traveling through matter in the positive x direction with momentum four-vector p^μ. We assume the particle interacts with the surrounding matter via photon emission, in which the particle then emits a photon at an angle θ relative to the x axis. We denote the photon's and particle's momentum four-vectors after the photon emission by p_γ^μ and p'^μ, respectively.

  We stress that in free space, the above spontaneous photon emission cannot simultaneously satisfy conservation of momentum and conservation of energy, and thus cannot occur. Photon emission can, however, occur in matter in the presence of massive nuclei, which account for conservation of momentum.

- We begin a quantitative analysis with conservation of four-momentum:

$$p'^\mu + p_\gamma^\mu = p^\mu \implies p'^\mu = p^\mu - p_\gamma^\mu.$$

  We then square the equality to get

$$(p'^\mu)^2 = (p^\mu)^2 + (p_\gamma^\mu)^2 - 2p^\mu \cdot (p_\gamma)_\mu. \tag{1.11}$$

- We write the four vectors in component form as $p^\mu = (E, c\mathbf{p})$ and $p_\gamma^\mu = (\hbar\omega, c\hbar\mathbf{k})$ and use the $(+---)$ metric for the four-vector inner product, which evaluates to

$$(p^\mu)^2 = p^\mu p_\mu = E^2 - c^2p^2 \equiv m^2c^4,$$

  where the last line uses the relativistic energy relation $E^2 = m^2c^4 + p^2c^2$. An analogous calculation for $(p'^\mu)^2$ reads

$$(p'^\mu)^2 = p'^\mu \cdot p'_\mu = E'^2 - c^2p'^2 \equiv m^2c^4,$$

  where E' and p' are the incident particle's energy and momentum after photon emission. We then substitute $(p^\mu)^2$ and $(p'^\mu)^2$ into Equation 1.11 to get

$$m^2c^4 = m^2c^4 + (p_\gamma^\mu)^2 - 2p^\mu \cdot (p_\gamma)_\mu \implies (p_\gamma^\mu)^2 = 2p^\mu \cdot (p_\gamma)_\mu. \tag{1.12}$$

  The photon four vector's square $(p_\gamma^\mu)^2$ is zero, which follows from e.g. $\omega = \hbar k$ and

$$(p_\gamma^\mu)^2 = p_\gamma^\mu \cdot (p_\gamma)_\mu = \hbar^2\omega^2 - c^2\hbar^2k^2 = \hbar^2\omega^2 - \hbar^2\omega^2 = 0.$$

  Together with Equation 1.12, the result $(p_\gamma^\mu)^2 = 0$ implies

$$0 \equiv \frac{1}{2}(p_\gamma^\mu)^2 = p^\mu \cdot (p_\gamma)_\mu \implies p^\mu \cdot (p_\gamma)_\mu = 0.$$

- We now take a closer look at the product $p^\mu \cdot (p_\gamma)_\mu$. Expanded out, this is

$$0 \equiv p^\mu \cdot (p_\gamma)_\mu = E\hbar\omega - c^2\hbar\mathbf{p} \cdot \mathbf{k} \implies \omega = c^2\frac{\mathbf{p} \cdot \mathbf{k}}{E}. \tag{1.13}$$

  Next, we turn to the general relativistic relationship

$$\frac{c\mathbf{p}}{E} = \beta\frac{\mathbf{v}}{|\mathbf{v}|}.$$

Derivation: We begin with $(cp)/E$, use the general identity $E = \gamma mc^2$, and perform some algebraic manipulations to get

$$\frac{cp}{E} = \frac{cp}{\gamma mc^2} = \frac{\sqrt{E^2 - m^2c^4}}{\gamma mc^2} = \sqrt{1 - \frac{m^2c^4}{\gamma^2 m^2 c^4}} = \sqrt{1 - \frac{1}{\gamma^2}} = \beta,$$

where the last equality follows from the identity

$$\gamma^2 = \frac{1}{1 - \beta^2}.$$

In terms of $\frac{c\mathbf{p}}{E} = \beta\frac{\mathbf{v}}{v}$, the photon's frequency in Equation 1.13 becomes

$$\omega = c^2\frac{\mathbf{p}\cdot\mathbf{k}}{E} = c\beta\frac{\mathbf{v}\cdot\mathbf{k}}{v} = v\cdot\frac{\mathbf{v}\cdot\mathbf{k}}{v} = \mathbf{k}\cdot\mathbf{v}. \tag{1.14}$$

Photon Dispersion Relation

- We now consider that photon emitted by the ionizing particle. In general, a photon obeys the dispersion relation

  $$\omega = ck = \frac{c_0}{n}k$$

  where n is the material's index of refraction. We then decompose $\mathbf{k}$ into components $\mathbf{k}_\parallel$ and $\mathbf{k}_\perp$ parallel and transverse to the direction of incident particle velocity in the form. The magnitude of the photon's wave vector k is then

  $$k = \sqrt{k_\parallel^2 + k_\perp^2},$$

  and the photon dispersion relation reads

  $$k^2 = k_\parallel^2 + k_\perp^2 = \frac{n^2\omega^2}{c_0^2}. \tag{1.15}$$

  We then write the ionizing particle's velocity as $\mathbf{v} = v\,\hat{\mathbf{e}}_\parallel$ (the particle velocity, naturally, only has a component in the direction to particle velocity), in which case the dot product in Equation 1.14 simplifies to

  $$\omega = \mathbf{k}\cdot\mathbf{v} = k_\parallel v \implies k_\parallel = \frac{\omega}{v}.$$

  We then substitute $k_\parallel = \omega/v$ into Equation 1.15 and solve for $k_\perp$, producing

  $$k_\perp^2 = \frac{n^2\omega^2}{c_0^2} - k_\parallel^2 = \frac{n^2\omega^2}{c_0^2} - \frac{\omega^2}{v^2},$$

  where v is the speed of the ionizing particle. After some algebra, $k_\perp$ comes out to

  $$k_\perp = \frac{\omega}{v}\sqrt{\frac{v^2}{c^2} - 1}. \tag{1.16}$$

Equation 1.16 motivates the separate analysis of two cases:

1. If $v > c$, i.e. if the ionizing particle's speed exceeds the speed of light in the material through which it travels, then $k_\perp \in \mathbb{R}$. In this case the photon emitted by the ionizing particle is real, with direction θ relative to the particle velocity axis given by

$$\tan\theta = \frac{k_\perp}{k_\parallel}.$$

We then use a trigonometric identity for $\cos\theta$, to rewrite this expression into the more insightful form

$$\cos\theta = \frac{1}{\sqrt{1+\tan^2\theta}} = \frac{1}{\sqrt{1+(k_\perp^2)/(k_\parallel^2)}} = \frac{1}{\sqrt{1+\frac{v^2}{c^2}-1}} = \frac{c}{v} = \frac{c_0}{nv} = \frac{1}{n\beta}.$$

This form of radiation is Cherenkov radiation, and is interesting, among other reasons, because the angle θ for photon emission is precisely determined the particle speed β. We will discuss Cherenkov radiation in Section 5.3 in the context of particle detection.

2. If $v < c$, then the photon wave vector component $k_\perp$ is imaginary. We then write

$$k_\perp = \frac{\omega}{v}\sqrt{\frac{v^2}{c^2}-1} = \frac{i\omega}{v}\sqrt{1-\frac{v^2}{c^2}}.$$

For convenience, we pack the entire right side into the constant y_0, which gives

$$k_\perp = \frac{i}{y_0}, \quad \text{where} \quad y_0 = \frac{v}{\omega}\frac{1}{\sqrt{1-\frac{v^2}{c^2}}}.$$

In this case, the photon represents sinusoidal electromagnetic radiation. If we let x point parallel to the particle velocity axis and y be the coordinate transverse to the particle axis, we can write the photon radiation as a plane wave of the form

$$e^{i(\mathbf{k}\cdot\mathbf{r}-\omega t)} = e^{i(k_x x + k_y y - \omega t)} = e^{i\left(\frac{w}{v}x + i\frac{y}{y_0} - \omega t\right)} = e^{i(\frac{w}{v}x-\omega t)}e^{-\frac{y}{y_0}}.$$

We are interested in the last term, i.e. e^{-y/y_0}; this represents electromagnetic radiation that decays exponentially with the distance y traveled by the photon in the direction transverse to the ionizing particle direction x. In this interpretation, y_0 represents a characteristic decay length,

$$y_0 = \frac{v}{\omega}\left(1-\frac{v^2}{c^2}\right)^{-1/2}.$$

Using the identities $\beta = \frac{v}{c_0}$ and $\gamma^2 = \frac{1}{1-\beta^2}$, we can write y_0 as

$$y_0 = \frac{\beta c_0}{\omega}\frac{1}{\sqrt{1-\beta^2 n^2}}.$$

Lesson: the range y_0 increases with β (at least in the relativistic regime), so an ionizing particle with larger β and thus larger y_0 interacts with more particles in the material it travels through.

1.2 Interaction of Photons with Matter

- Photons experience three important interactions in matter. These are:

  1. the photoelectric effect,
  2. Compton scattering, and
  3. pair production.

  Photons interact quite differently with matter than charged particles. The reason lies in the photon's quantum nature—at least in the photoelectric effect and pair formation, a photon loses all of its energy in a single discrete process and then disappears, while a classical particle would lose energy continuously before coming to a stop. As we will derive below, because of energy loss in discrete quanta, a photon beam exhibits exponential intensity attenuation in matter of the form

  $$I = I_0 e^{-\mu x},$$

  where x is the distance traveled through matter and μ is a material-specific attenuation constant.

- Finally, we note that the scattering cross sections for the above photon processes are much smaller than cross sections for typical charged particle processes. As a result, photons tend to travel farther through matter than charged particles.

1.2.1 Scattering Cross Section and Exponential Attenuation

- Consider a beam of photons with energy $h\nu$ incident on a particle detector. The photon scattering cross section σ (units of area) encodes the likelihood that an incident photon will observably interact with the particle detector (instead of passing through undetected).

  For a thin detector segment of thickness $\mathrm{d}x$, the probability that a single incident photon interacts with the detector in terms of scattering cross section as

  $$\mathrm{d}P_0 = \sigma \frac{\mathrm{d}N_\mathrm{e}}{\mathrm{d}S},$$

  where $\frac{\mathrm{d}N_\mathrm{e}}{\mathrm{d}S}$ is the surface density of electrons in the detector. To account for the detector's width $\mathrm{d}x$, we rewrite the electron density in the form

  $$\frac{\mathrm{d}N_\mathrm{e}}{\mathrm{d}S} = \frac{\mathrm{d}N_\mathrm{e}}{\mathrm{d}V}\,\mathrm{d}x = \frac{\mathrm{d}(ZN_\mathrm{at})}{\mathrm{d}V}\,\mathrm{d}x = Z\frac{\mathrm{d}N_\mathrm{at}}{\mathrm{d}(m/\rho)}\,\mathrm{d}x = Z\rho\frac{N_\mathrm{A}}{M_\mathrm{m}}\,\mathrm{d}x,$$

  where N_a is the number of atoms in the detector, while Z, ρ, and M_m are the atomic number, density and molar mass of the material in the detector and N_A is Avogadro's number. The probability that a single photon interacts with the detector is then

  $$\mathrm{d}P_0 = \sigma\frac{\mathrm{d}N_\mathrm{e}}{\mathrm{d}S} = \sigma Z\rho\frac{N_\mathrm{A}}{M_\mathrm{m}}\,\mathrm{d}x \equiv \mu\,\mathrm{d}x,$$

  where we have defined the attenuation constant

  $$\mu \equiv \sigma Z\rho\frac{N_\mathrm{A}}{M_\mathrm{m}}.$$

In terms of the single-photon interaction probability $\mathrm{d}P_0$, the fraction $\mathrm{d}N_{\mathrm{int}}$ of photons interacting with the detector segment in a beam of N_γ incident photons is

$$\mathrm{d}N_{\mathrm{int}} = N_\gamma \cdot \mathrm{d}P_0 = N_\gamma \mu \, \mathrm{d}x.$$

The number of photons in the incident beam decreases with each photon-detector interaction. It follows that the rates of change of photon number $\mathrm{d}N_\gamma$ and interaction number $\mathrm{d}N_{\mathrm{int}}$ are equal and opposite, i.e.

$$\mathrm{d}N_\gamma = -\,\mathrm{d}N_{\mathrm{int}} \implies \mathrm{d}N_\gamma = -\mu N_\gamma \, \mathrm{d}x.$$

The last equation for the number of photons N_γ in the beam has the well-known exponential solution

$$N(x) = N_0 e^{-\mu x},$$

where I have dropped the subscript γ for conciseness. This solution is the characteristic exponential attenuation of a photon beam in matter quoted in the introduction.

- Finally, we note that if multiple processes are possible for photon interaction in the detector, we must write the total attenuation constant μ_{tot} as a sum over the individual μ_i for each process, where the i-th process is parametrized by its own cross section σ_i. This photon-interaction picture then reads

$$\mu_{\mathrm{tot}} = \sum_i \sigma_i Z \rho \frac{N_{\mathrm{A}}}{M_{\mathrm{m}}} \qquad \text{and} \qquad N_{\mathrm{tot}}(x) = N_0 e^{i\mu_{\mathrm{tot}} x}.$$

1.2.2 Photoelectric Effect

- In the photoelectric effect, a photon incident on an atom ejects an electron from the atom. The atom absorbs the entire photon energy, while the photon itself disappears in the interaction. The energy gained by the emitted electron in the interaction is

$$E_{\mathrm{e}} = h\nu - W,$$

where W is a material-dependent property called the *work function*; it encodes the binding energy between the electron and its parent atom. Work functions are typically of the order of a few electron volts; some representative values are given in the table below

Element	W [eV]
Sodium Na	2.28
Zinc Zn	4.31
Silver Ag	4.73
Platinum Pt	6.35

- Without derivation, a rough approximation for the photon scattering cross section in a material with atomic number Z takes the form

$$\sigma_{\mathrm{pe}} \propto \frac{Z^n}{E_\gamma^{7/2}},$$

where n is an empirically-determined constant in the range $n = 4$ to $n = 5$. Key takeaways here is that the cross section decreases rapidly with increasing photon energy (i.e. higher-energy photons travel farther in material) and increases rapidly with increasing atomic number (large-Z materials are good photon absorbers).

1.2.3 Compton Scattering

- Compton scattering refers to a photon scattering from an atomic electron. Of the three photon processes mentioned in the beginning of this section, it is the only process in which the photon does not loose all of its energy in a single discrete packet and disappear.
- Consider a photon with initial energy $h\nu$ traveling along the z axis an scattering from an electron, initially at rest. The photon scatters with the new energy $h\nu'$ at an angle θ relative to the direction of incidence, while the electron gains kinetic energy T_e. Note that this process is possible only in the presence of a nucleus, which accounts for conservation of momentum.
- The initial photon and electron four vectors are

$$p_\gamma^\mu c = (h\nu, 0, 0, h\nu) \qquad \text{and} \qquad p_\mathrm{e}^\mu c = (mc^2, \mathbf{0}),$$

where m denotes the electron mass. The final photon four-vector is

$$p_\gamma'^\mu c = (h\nu', h\nu' \sin\theta, 0, h\nu' \cos\theta),$$

while the final electron four vector is

$$p_\mathrm{e}'^\mu c = \left(\sqrt{p_\mathrm{e}^2c^2 + m^2c^4}, -p_\mathrm{e}c\sin\phi, 0, p_\mathrm{e}c\cos\phi\right),$$

where ϕ denotes the angle between the direction of the scattered electron and the direction of the incident photon and p_e is the magnitude of electron momentum after scattering. Conservation of energy requires the relationship

$$mc^2 + h\nu = h\nu' + \sqrt{p_\mathrm{e}^2c^2 + m^2c^4}. \tag{1.17}$$

Meanwhile, conservation of momentum in the z direction requires

$$h\nu = h\nu'\cos\theta + p_\mathrm{e}c\cos\phi, \tag{1.18}$$

while conservation of momentum in the x direction requires

$$h\nu'\sin\theta = p_\mathrm{e}c\sin\phi. \tag{1.19}$$

- Our goal is to solve for the final photon frequency ν' in terms of the initial frequency ν and photon scattering angle θ. To do this, we solve for $\sin\phi$ in Equation 1.19, substitute this into Equation 1.18, solve for p_e, and substitute p_e into Equation 1.17. The result comes out to

$$h\nu' = \frac{h\nu}{1 + \alpha(1 - \cos\theta)}, \quad \text{where } \alpha \equiv \frac{h\nu}{m_\mathrm{e}c^2}. \tag{1.20}$$

We stress that γ is not the fine structure constant, but the dimensionless ratio of initial photon energy to electron rest energy. In terms of the photon's de Broglie wavelength $\lambda = h/p = ch/(h\nu) = c/\nu$, Equation 1.20 reads

$$\frac{hc}{\lambda'} = \frac{(hc)/\lambda}{1 + \frac{hc}{m_\mathrm{e}c^2}(1 - \cos\theta)}.$$

Finally, we solve for photon's post-scattering wavelength λ' and introduce the electron Compton λ_e to get

$$\lambda' = \lambda + \frac{h}{m_\mathrm{e}c}(1 - \cos\theta) \equiv \lambda + \lambda_\mathrm{e}(1 - \cos\theta), \quad \text{where } \lambda_\mathrm{e} \equiv \frac{h}{m_\mathrm{e}c}.$$

- We now find the electron post-scattering kinetic energy T_e from conservation of energy in Equation 1.17:

$$mc^2 + h\nu = h\nu' + E_\mathrm{e} \implies T_\mathrm{e} \equiv E_\mathrm{e} - mc^2 = h\nu - h\nu'.$$

  We then substitute in Equation 1.20 for $h\nu'$ and divide through by electron rest energy to get

$$T_\mathrm{e} = h\nu - h\nu' \implies \frac{T_\mathrm{e}}{m_\mathrm{e}c^2} = \frac{\alpha^2(1-\cos\theta)}{1+\alpha(1-\cos\theta)}.$$

  The normalized electron energy $T_\mathrm{e}/(m_\mathrm{e}c^2)$ increases monotonically from $\theta = 0$ to $\theta = \pi$, where θ is the photon's scattering angle. The maximum electron energy occurs when $\theta = \pi$, i.e. when the photon perfectly backscatters (i.e. a head-on collision). The maximum electron energy at $\theta_\mathrm{max} = \pi$ is then

$$\frac{T_\mathrm{e}^\mathrm{max}}{m_\mathrm{e}c^2} = \frac{2\alpha^2}{1+2\alpha}.$$

- Finally, we define the quantity s as the ratio of post-scattering electron energy and initial photon energy; this is

$$s \equiv \frac{T_\mathrm{e}}{h\nu} = \frac{m_\mathrm{e}c^2}{h\nu}\frac{\alpha^2(1-\cos\theta)}{1+\alpha(1-\cos\theta)} \leq 1,$$

  and is less than or equal to one by conservation of energy. The maximum value of s, like T_max, occurs at $\theta_\mathrm{max} = \pi$ and equals

$$s_\mathrm{max} = s(\pi) = \frac{m_\mathrm{e}c^2}{h\nu}\frac{2\alpha^2}{1+2\alpha} = \frac{1}{\alpha}\frac{2\alpha^2}{1+2\alpha} = \frac{2\alpha}{1+2\alpha}.$$

  Without derivation, we quote that the plot of Compton scattering cross section $\frac{\mathrm{d}\sigma_\mathrm{C}}{\mathrm{d}s}$ with respect to s has a steep maximum at $s = s_\mathrm{max}$—this peak is called the Compton scattering cross section's *Compton edge*.

- Without derivation, the Compton scattering cross section's angular distribution for photon scattering from a single free electron is well-approximated by the *Klein–Nishina formula*

$$\frac{\mathrm{d}\sigma_\mathrm{C}}{\mathrm{d}\Omega} = \frac{r_\mathrm{e}^2}{2}\frac{1}{\left[1+\gamma(1-\cos\theta)\right]^2}\left(1+\cos^2\theta + \frac{\alpha^2(1-\cos\theta)^2}{1+\alpha(1-\cos\theta)}\right).$$

  At low incident photon energies (e.g. $h\nu \sim 1\,\mathrm{kV}$), the scattering is approximately isotropic, i.e. the photon is equally likely to scatter in all spatial directions. As photon energy increases, forward scattering grows more dominant.

1.2.4 Pair Production

- Pair production refers to a photon decaying into an electron-positron pair. There are few important restrictions governing pair production; we begin with conservation of energy, which for a photon of energy $h\nu$ decaying into a positron and electron reads

$$h\nu = E_+ + E_- = 2m_\mathrm{e}c^2 + T_+ + T_-,$$

where E_+ and E_- denote the positron and electron energies, respectively. The above relationship immediately establishes a photon energy threshold of

$$h\nu \geq 2m_e c^2 \approx 1.02\,\text{MeV}.$$

In other words, pair production can occur only for photons with energy $h\nu \geq 2m_e c^2$; if the photon's energy were less than $2m_e c^2$, the photon would not carry enough energy to create the electron and position rest masses.

- Second, we note that pair production process is possible only in the presence of a heavy nucleus, which accounts for conservation of momentum. The pair production process is impossible in free space.

  To see why pair production violates conservation of energy in free space, consider a photon of energy $h\nu$ decaying into an electron and positron, which fly off with momentum p at symmetric angles $\theta_\pm \equiv \pm\theta$ relative to the photon's direction of incidence. Conservation of energy for this process requires

$$h\nu = 2\sqrt{m_e^2 c^4 + c^2 p^2},$$

  while conservation of momentum requires

$$p_\gamma = \frac{h\nu}{c} = 2p\cos\theta \implies h\nu = 2cp\cos\theta.$$

  We then equate the two expressions for $h\nu$, square both sides and rearrange to get

$$2\sqrt{m_e^2 c^4 + c^2 p^2} = 2cp\cos\theta \implies m_e^2 c^4 = c^2 p^2(\cos^2\theta - 1).$$

  Since $\cos^2\theta$ is always less than or equal to one, the quantity in parentheses is either negative or equal to zero for all θ, which implies the electron rest mass $m_e c^2$ would be less than or equal to zero, which is non-physical. We conclude pair production in empty space is impossible.

- Without derivation, the distribution of the pair production cross section of electron/positron energy is approximately given by

$$\frac{\mathrm{d}\sigma_{\text{pair}}}{\mathrm{d}E_-} = \frac{\mathrm{d}\sigma_{\text{pair}}}{\mathrm{d}E_+} \propto \frac{Z}{(h\nu)^3}\left(E_+^2 + E_-^2 + \frac{2}{3}E_+E_-\right),$$

  where Z is the atomic number of the material through which the photons travel.

Summary of Photon-Matter Interactions

- The photoelectric effect is the dominant photon-matter interaction at low photon energies (e.g. $h\nu \ll 2m_e c^2$).
- The Compton effect dominates at mid-range energies $h\nu \lesssim 2m_e c^2$
- Pair production dominates above the threshold energy $m_e c^2 \approx 1.02\,\text{MeV}$
- Although the above three regimes provide a general trend, note that the likelihoods for the photoelectric effect and pair production in a given material depend strongly on the material's atomic number Z.

  For orientation, a 1 MeV photon reaches about 1 cm in lead and 100 m in air.

2 Cylindrical Gas-Based Detectors

- Gas-based detectors work on the following basic principle: an external housing, generally with either cylindrical or rectangular geometry, contains a mixture of noble and organic gases (for example a mixture of 90% argon and 10% methane known as P-10), and a kilovolt-order potential difference is established across the gas chamber. Incident particles passing through the gas deposit energy, freeing electron-ion pairs which are then accelerated by the potential difference to opposite housing faces and produce a measurable current pulse indicating the presence of the initial incident particle.
- We will consider in detail gas-based detectors with *cylindrical* geometry. In cylindrical detectors, the outer cylindrical housing is grounded and serves as a cathode, while a thin wire inside the chamber, along the cylinder's central axis, is held at a positive potential relative to ground and serves as an anode. This setup creates a cylindrically-symmetric electric field within the gas chamber pointing radially outward from the inner anode wire.
- Let R and r_0 denote the radius of the outer chamber and anode wire, respectively, and let U_0 denote the potential difference between the anode wire and cathode surface. Quoting from electrostatics, the electric field in the cylindrical chamber a radial distance r from the cylinder axis is

$$\mathbf{E}(r) = \frac{U_0}{\ln(R/r_0)} \frac{1}{r} \hat{\mathbf{e}}_r. \tag{2.1}$$

  The corresponding potential $U(r)$ in the chamber is

$$\phi(r) = -\frac{U_0}{\ln(R/r_0)} \ln \frac{r}{r_0}. \tag{2.2}$$

  Finally, again from electrostatics, the chamber's capacitance per unit length is

$$\frac{C}{L} = \frac{2\pi\epsilon_0}{\ln(R/r_0)}.$$

- Detecting an ionizing event is a two-step process:
  1. An initial ionizing particle flies into detector somewhere in the range $r \in (r_0, R)$ and creates a *small* number of primary ions.
  2. Primary positive ions drift toward the outer cathode surface and primary electrons toward the anode wire. When the primary electrons are near the anode, where the $E \sim 1/r$ electric field is strong, they gain enough energy to cause secondary ionization, which creates a *large* number of ions. Only the *secondary* ions are numerous enough to create a measurable signal.

2.1 Working Regimes of Cylindrical Detectors

- We now consider how the number N of detected ion pairs resulting from a single incident ionizing particle in a cylindrical detector changes with the potential difference U_0 between the anode and cathode.
- **Small Voltage:** For very small U_0, primary ions recombine inside the gas chamber before reaching the anode, and the number of detected ions N is negligible. Increasing U_0 causes more primary ions to reach the anode, increasing N.

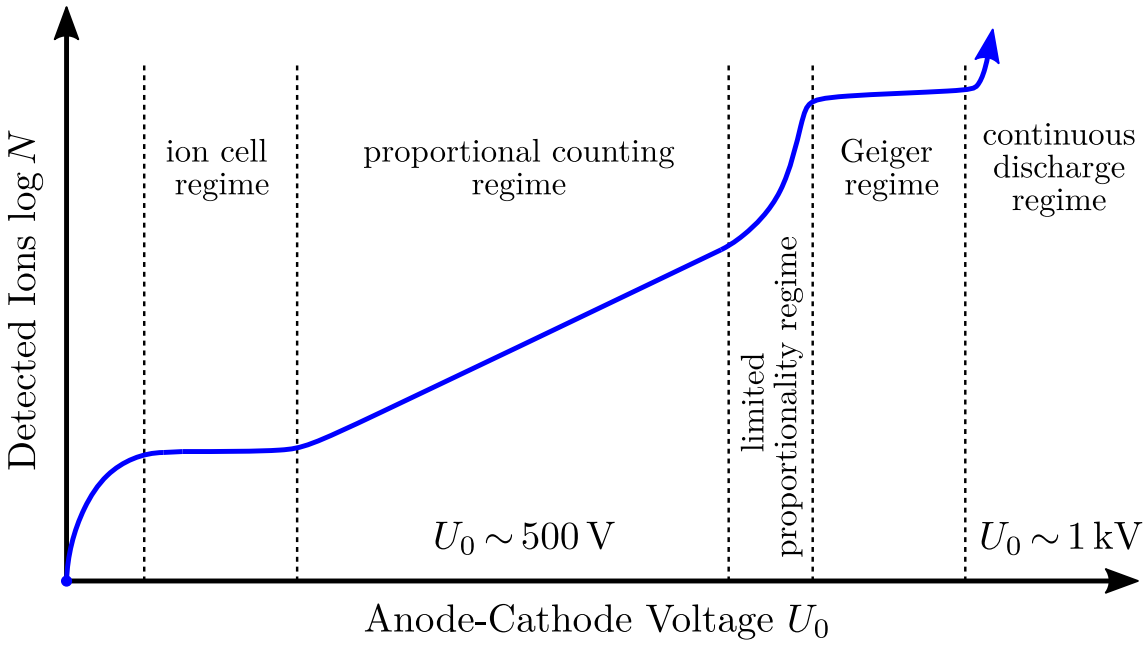

Figure 1: Working regimes of a cylindrical gas-based detection chamber showing the number of detected ion pairs N (in log scale) as a function of the detector's anode-cathode voltage U_0. Adapted from [Doug Sim. Practical Gaseous Ionisation Detection Regions. Accessed June 2021. https://en.wikipedia.org/wiki/File:Detector_regions.gif] under a CC BY-SA 3.0 unported license.

- **Ion cell regime:** Once U_0 is large enough to prevent recombination, all primary ions reach the anode wire; in this regime N saturates at a constant value with respect to U_0. In this regime U_0 is still too small to cause secondary ionizations. Only primary ions are detected.
- **Proportional counting regime:** The proportional counting regime begins when U_0 is large enough to accelerate primary ions to energies required for secondary ionization—this typically occurs for $U_0 \sim 500\,\mathrm{V}$. In this regime the majority of detected ions result from secondary ionization.

  Keep in mind that the "proportionality" in "proportional counting regime" refers to proportionality between total number of detected ions N and the number of primary ions, say N_0, and *not* to proportionality between N and U_0—N increases rapidly with increasing U_0, since larger U_0 leads to more secondary ionization.

  A proportional counter works because the detector's electrical signal amplitude (which is proportional to the number of detected anode ions N) is proportional to the energy deposited E_{dep} by primary particles in the detector (which is proportional to the number of initial particles N_0). Detector signal amplitude, via N and then E_{dep}, is thus proportional to N_0.
- **Limited proportionality regime:** In this regime, $N(N_0)$ is nonlinear, so the regime is thus not particularly useful for particle detection—we can't predict the number of primary ionized particles from the total number of detected ionized particles.

  The nonlinear dependence of N on N_0 results from the large number of secondary ionized particles that accumulate in the detector chamber shadowing the electric field

of the internal anode. Basically, a ton of charge accumulates in the detector chamber, which shadows the electric field arising from the detector anode and cathode.

- **Geiger-Müller regime:** In this regime the voltage V_0 is large enough that ions accelerate to large enough energies to excite the gas atoms (or molecules) into high-energy excited states—the atoms then emit photons in the relaxation process. These photons can travel quite far through the detector, since photons have long range. The photons travel through the gas and free (e.g. via the photoelectric effect) electrons throughout the detector's volume. Because of these long-range photons, the entire volume of the detector is electrified (ionized) (and not just the portion of the detector near the anode wire).
- **Dielectric breakdown:** in this regime U_0 has grown large enough to cause dielectric breakdown in the detector gas. The gas itself becomes conducting, causing a surge in current throughout the detector.

2.1.1 Proportional Counting Regime

Multiplication Factor

- In the proportional counting regime the number N of all detected particles is proportional to the number of primary ionized particles N_0.

  Let σ be the cross section for creation of an ion pair in the detector (for scattering of a freed ion from a single gas atom) and let n_{at} be the number density of gas atoms in the detector. For orientation, a typical value is roughly $n_{\text{at}} \approx 2.7 \cdot 10^{19}\,\text{cm}^3$. In terms of σ and n_{at}, the probability of an ionizing particle producing secondary ions per unit distance x traveled through the detector is

  $$\frac{\mathrm{d}P}{\mathrm{d}x} = \alpha = \sigma n_{\text{at}}.$$

  In terms of α, if $N(x)$ ions are currently in the gas chamber at position x the number $\mathrm{d}N$ of secondary ions freed by an ionizing particle is

  $$\mathrm{d}N(x) = N(x)\alpha\,\mathrm{d}x \implies N(x) = N_0 e^{\alpha x}, \tag{2.3}$$

  where N_0 is the initial number of free ions in the gas chamber.

  Lessons: (i) the number of freed secondary ions increases exponentially with the distance x traveled by an initial incident particle through the detector (because each freed secondary ion can free more ions), and (ii) more importantly, the total number N of secondary ions is proportional to the number of primary ions N_0, hence the name *proportional counting regime*.

  In practice, N_0 would be the number of primary ions freed by an incident ionizing particle (which we wish to detect) and N would be the number of secondary particles reaching the anode wire.

- Note that only secondary electrons cause further ionizations, because only electrons near the anode wire where the $E \sim 1/r$ electric field is strong will have sufficient energy to cause further ionizations.
- Generalizations: For example, $\alpha = \alpha(\sigma)$, while $\sigma = \sigma(E)$ where E is the energy of a secondary ionizing electron. This energy is proportional the electric field strength

between the anodes, which in turn depends on the radial position r in the detector, so Equation 2.3 should generalize to

$$N(x) = N_0 \exp\left(\int \alpha(x)\,\mathrm{d}x\right),$$

where the integral runs over the full path followed by a primary ionizing electron through the detector (for example from the average point of initial ionization $r^* \lesssim R$ to the point of secondary ionization at $r \sim r_0$).

- The quantity

$$M \equiv \exp\left(\int \alpha(x)\,\mathrm{d}x\right) \tag{2.4}$$

is called the gas detector's *multiplication factor*, and encodes how many secondary electrons will reach radial position x for a given number of primary electrons N_0.

Position of Secondary Ionizations

- Let r^* denote the position of secondary ionization, where a primary electron accelerating towards the anode first gains enough energy to produce secondary ions. The energy gained by a secondary electron during acceleration from r^* to the anode wire at $r = a$ is

$$\Delta W_\mathrm{E} = \int_{\mathbf{r}^*}^{\mathbf{r}_0} \mathbf{F}_\mathrm{E} \cdot \mathrm{d}\mathbf{r} = -e_0 \int_{\mathbf{r}^*}^{\mathbf{r}_0} \mathbf{E} \cdot \mathrm{d}\mathbf{r}.$$

We then substitute in the cylindrical electric field from Equation 2.1, use the minus sign to switch the limits of integration, and assume $\mathrm{d}\mathbf{r} \parallel \hat{\mathbf{e}}_r$ to get

$$\Delta W_\mathrm{E} = +e_0 \int_{\mathbf{r}_0}^{\mathbf{r}^*} \frac{U_0}{\ln(R/r_0)} \frac{\hat{\mathbf{e}}_r \cdot \mathrm{d}\mathbf{r}}{r} = e_0 \int_{r_0}^{r^*} \frac{U_0}{\ln(R/r_0)} \frac{\mathrm{d}r}{r} = e_0 U_0 \frac{\ln(r^*/r_0)}{\ln(R/r_0)}.$$

To cause secondary ionization, the energy ΔW_E gained by a secondary electron must exceed the average energy, say w_i, required to ionize a gas atom in the detector. In symbols, this condition reads

$$\Delta W_\mathrm{E} > w_\mathrm{i} \implies \ln\frac{r^*}{r_0} > \frac{w_\mathrm{i}}{e_0 U_0} \ln\frac{R}{r_0}.$$

We then solve for r^* and get

$$r^* > r_0 \exp\left(\frac{w_\mathrm{i}}{e_0 U_0} \ln\frac{R}{r_0}\right). \tag{2.5}$$

For orientation, w_i is typically of the order 15 to 30 eV. As an example, for $R \sim 2\,\mathrm{cm}$ and $r_0 \sim 0.1\,\mathrm{mm}$, $w_\mathrm{i} \sim 15\,\mathrm{eV}$ and $U_0 \sim 200\,\mathrm{V}$ we have

$$\ln\frac{r^*}{r_0} > \frac{15\,\mathrm{eV}}{200\,\mathrm{eV}} \ln 200 \implies r^* \gtrsim 1.5 r_0.$$

Lesson: ionization must occur far enough away from anode wire position r_0 for secondary ions to produce more ions.

- (What is the reasoning here?) to satisfy the $R \geq r^* \geq r_0$ condition we also require

$$\ln\frac{R}{r^*} \geq \frac{w_\mathrm{i}}{e_0 U_0} \ln\frac{R}{r_0} \implies r^* \leq R \exp\left(-\frac{w_\mathrm{i}}{e_0 U_0} \ln\frac{R}{r_0}\right),$$

which comes out about $r^* \lesssim 0.7R$ for typical values of w_i, U_0, and R/r_0.

We conclude that primary ionization should occur roughly in the range $1.5r_0 \lesssim r^* \lesssim 0.7R$ for secondary ionization to occur.

Avalanche of secondary ionizations

- In practice, the detector is designed to produce an avalanche of secondary ionizations so as to maximize the number of electrons reaching the anode wire and thus increase the strength of the resulting detected electrical signal. As a simple model, consider one initial electron e_0 initially in the detector; this electron ionizes a gas atom and produces a second electron e_1. Electron e_0 and e_1 continue through the gas and each produce second electrons $e_a^{(2)}$ and $e_b^{(2)}$, the next round of ionizations produces $e_a^{(3)}$, $e_b^{(3)}$, $e_c^{(3)}$, $e_d^{(3)}$, and so on. The total number N of electrons in the gas chamber after n ionizations comes out to

$$N(n) = 2^{n-1}.$$

For an avalanche with large n, the initial ionization must occur far enough radially outward from the anode wire for secondary electrons to have room to accelerate; this idea motivates the following condition for position of first ionization r_1^*:

$$r^* \lesssim R \exp\left(-\frac{w_i}{e_0 U_0} \ln \frac{R}{r_0}\right).$$

Second ionizations necessarily occur further radially inward than the first ionization, the so the second ionization must obey

$$r_2^* < r_1^* \exp\left(-\frac{w_i}{e_0 U_0} \ln \frac{R}{r_0}\right) = R \exp\left(-\frac{2w_i}{e_0 U_0} \ln \frac{R}{r_0}\right).$$

Generalizing, the position of the n-th ionization must satisfy

$$r_n^* < R \exp\left(-\frac{nw_i}{e_0 U_0} \ln \frac{R}{r_0}\right).$$

Combining the above condition with Equation 2.5, a requirement on r_n^* for an avalanche of secondary ionizations to occur is

$$r_0 \exp\left(\frac{w_i}{e_0 U_0} \ln \frac{R}{r_0}\right) < r_n^* < R \exp\left(-\frac{nw_i}{e_0 U_0} \ln \frac{R}{r_0}\right).$$

To create $N \sim 5 \cdot 10^3$ ions from a single initial ion, which corresponds to $n \sim 12$ generations of secondary ionizations, the above condition (for typical values of w_i, U_0, and R/r_0) requires about

$$1.5r_0 \lesssim r_n^* \lesssim 1.7r_0.$$

Lesson: most of the secondary ionizations occur for r_n^* in a very close range to the inner anode wire, where electrons have enough energy to cause further ionizations.

2.1.2 Geiger-Müller Regime

- Electrons (generally from secondary ionizations)) excite gas atoms or molecules into excited states with a given probability (say η. The gas atoms/molecules then emit photons in the relaxation process to lower-energy states.

Suppose an incident ionization particle frees N_0 primary electrons in the initial ionization. These N_0 primary electrons then produce MN_0 secondary electrons after passing through the detector, where M is the detector's multiplication factor (e.g. from Equation 2.4). These secondary electrons excite $\eta M N_0$ atoms, which emit photons that in turn free a number of photoelectrons proportional to MN_0. As an approximate model, we will assume each excited atom emits exactly one photon, and each photon causes frees exactly one photoelectron somewhere in the detector via the photoelectric effect, so that the number of freed photoelectrons is also $\eta M N_0$.

The secondary ionization process then continues and produces further ionizations: the $\eta M N_0$ photoelectrons produce $M \cdot (\eta M N_0)$ electrons, which in turn produce $\eta M \cdot (\eta M N_0)$ photoelectrons. Continuing the pattern, the total sum of ionized electrons is then

$$N_{\text{tot}} = MN_0 + \eta M^2 N_0 + \eta^2 M^3 N_0 + \cdots = MN_0 \left[1 + \eta M + \eta^2 M^2 + \cdots\right].$$

This is a geometric series, which for n terms sums to

$$N_{\text{tot}}(n) = MN_0 \left(\frac{1 - (\eta M)^{n+1}}{1 - \eta M}\right).$$

This expression diverges for large N as long as as $\eta M \gtrsim 1$. Quoting from lecture, a typical multiplication factor in a GM tube is of the order $M \sim 10^3$, while atomic excitation probabilities are of the order $\eta \sim 10^{-3}$. Thus $\eta M \sim 1$ in a GM tube and $N_{\text{tot}} \to \infty$ for large n. Lesson: our (very approximate) model produces a theoretical prediction that agrees with the observed behavior of a GM tube rapidly filling with electrons throughout its entire volume.

2.2 Mechanisms of Ionization

- The simplest ionization mechanism is *direct ionization*. Schematically, for a particle P ionizing an atom of element X, the direct ionization process reads

$$X + P \rightarrow X^+ + e^- + P.$$

  Naturally, ionization can occur only if the P particle's energy exceeds the atom's ionization energy. However, because particle-atom energy transfers in gas are usually less than typical ionization energies, the principle mechanism for ionization in gas is *not* direct ionization.

  Instead, the principle ionization mechanism in gas-based detectors is called *Penning ionization*. In Penning ionization, we consider an ionizing particle P incident on a *mixture* of X and Y gas atoms. First, the incident P particle deposits enough energy to excite (but not ionize) an atom of element X to a higher energy state. This reads

$$X + P \rightarrow X^* + P.$$

  Second, the excited X^* atom relaxes to the ground state and in the process ionizes an atom of type Y, which has a lower ionization energy. This reads

$$X^* + Y \rightarrow X + Y^+ + e^-.$$

- An opposite process of ionization is also possible, in which an cation (positive) gas atom and free electron combine to produce a neutral gas atom. This process is called *recombination*. Naturally, recombination is undesirable in detectors, since charge ions are required to produce a measurable electrical signal from the detector.

- Some example recombination processes include...

  1. Direct recombination, in which a cation X^+ and electron combine and emit a photon. This process reads

$$X^+ + e^- \rightarrow X + h\nu.$$

  2. Recombination of atomic or molecular ions, in which the negative electron is replaced by an atomic or molecular anion Y^-. This reads

$$X^+ + Y^- \rightarrow XY + h\nu.$$

- A final relevant mechanism is *electron capture ionization*, which reads

$$X + e^- \rightarrow X^- + h\nu.$$

  In other words, a neutral gas atom X absorbs an electron, producing an anion X^-, and emits a photon. Electron capture occurs in highly electronegative elements, in which the absorption of an electron is energetically favorable.

  Electron capture ionization is undesirable in gas-based detectors, since it reduces the electron count in the detection chamber. For this reason, the gas used in gas-based detectors is chosen to have low-electronegativity.

  For this reason (among others) gas-based detectors generally use noble gas, often argon and/or neon. Additionally, detectors often include a small percentage of organic gas (such as carbon dioxide, methane, etc...), which capture excess photons. Photon capture is desirable in proportional counting detectors to avoid the Geiger-Müller regime caused by photoelectrons freed by excess photons.

2.3 Energy Resolution and Number of Ion Pairs

- First, we stress again that ionization is a stochastic process. In other words, an identical particle with identical energy and direction sent through a gas chamber will not always produce the same number of ion pairs. Instead the number N of ion pairs freed by a single ionizing particle is a random variable, which we will assume is distributed according a Poisson distribution with expected value μ. In symbols,

$$\frac{\mathrm{d}P}{\mathrm{d}N} = \frac{\mu^N e^{-\mu}}{N!}.$$

As a review from statistics, we will now show that the random variable N's expectation value is indeed μ. By definition

$$\langle N \rangle \equiv \sum_{N=0}^{\infty} N \frac{\mathrm{d}P}{\mathrm{d}N} = \sum_{N=0}^{\infty} N \frac{\mu^N e^{-\mu}}{N!} = 0 + \sum_{N=1}^{\infty} \frac{\mu^N e^{-\mu}}{(N-1)!}$$

We evaluate the sum by introducing a new index $k \equiv N - 1$ and then recognizing the Taylor series for the exponential function. This gives

$$\langle N \rangle = \sum_{k=0}^{\infty} \frac{\mu^{k+1} e^{-\mu}}{k!} = \mu e^{-\mu} \sum_{k=0}^{\infty} \frac{\mu^k}{k!} = \mu e^{-\mu} e^{+\mu} = \mu.$$

Without derivation, a calculation of N's variance σ_N^2 using a similar procedure with $\langle N^2 \rangle$ instead of $\langle N \rangle$ produces

$$\langle N^2 \rangle = \mu^2 + \mu \implies \sigma_N^2 = \langle N^2 \rangle - \langle N \rangle^2 = \mu^2 + \mu - \mu^2 = \mu.$$

Finding Number of Ion Pairs

- Assuming an incident ionizing particle deposits energy E_{dep} in detector. The average number of freed ion pairs $\langle N \rangle$ can be related to E_{dep} in terms the average energy w needed to free a single ion pair, i.e.

$$\langle N \rangle = \frac{E_{\mathrm{dep}}}{w}.$$

Interesting note: w is similar for a wide range of different gases and ionizing particles. A good global approximation is $w \approx 30\,\mathrm{eV}$. Note also that w is generally larger than the ionization energy E_{i}, since many other processes occur in the gas besides direct ionization, which all take up energy.

In any case, the number of ion pairs N can thus be used to measure the energy deposited by a particle in a detector via

$$\langle E_{\mathrm{dep}} \rangle = wN.$$

Because of the stochastic ion creation process, the estimated deposited energy E_{dep} for a given number of freed ions N is not exact, but an expected value. Fluctuations in E_{dep} are given by

$$\frac{\sigma_E}{E_{\mathrm{P}}} = \frac{\sigma_N}{N}.$$

If N is Poisson-distributed, then $\sigma_N = \sqrt{N}$, and so

$$\frac{\sigma_E}{E_{\mathrm{dep}}} = \frac{\sigma_N}{N} = \frac{\sqrt{N}}{N} = \frac{1}{\sqrt{N}} = \sqrt{\frac{w}{E_{\mathrm{dep}}}}.$$

Note that relative energy resolution improves (decreases) with increasing particle energy. Keep in mind that this expression holds only as long as the number of ion pairs freed in the detector is a Poisson-distributed random variable, which requires ionization events are independent.

Special Case: All Energy Left in Detector

- If a particle deposits its full energy in the detector, it will naturally come to a full stop inside the detector volume. As the particle slows and looses appreciable energy with each ionization (appreciable relative to its small remaining kinetic energy), ionization events are no longer independent or Poisson distributed, and the above analysis must be generalized.

  Again assume an incident particle deposits energy E_{dep} in the detector, and that some energy is used for direct ionization and some for Penning ionization. We write this as

  $$E_{\text{dep}} = N_{\text{i}} E_{\text{i}} + N_X E_X,$$

  where E_{i} is the gas's ionization energy and E_X is the energy required for Penning ionization. We then solve for the the number of ionized particle N_{i} to get

  $$N_{\text{i}} = \frac{E_{\text{dep}} - N_X E_X}{E_{\text{i}}}.$$

  We now aim to find the fluctuations in $\sigma_{N_{\text{i}}} \equiv \sigma_{\text{i}}$. We will use the first-order approximation that fluctuations σ_y for $y = f(x)$ are

  $$\sigma_y = \left|\frac{\partial f}{\partial x}\right| \sigma_x,$$

  which leads to

  $$\sigma_{N_{\text{i}}} = \left|\frac{\partial N_{\text{i}}}{\partial N_X}\right| \sigma_X = \frac{E_X}{E_{\text{i}}}\sqrt{N_X},$$

  where we have used the Poisson distribution result $\sqrt{N_X} = \sigma_X$ (which still holds for Penning ionization?). We then return to the equation $E_{\text{dep}} = N_{\text{i}} E_{\text{i}} + N_X E_X$ and solve for $\sqrt{N_X}$ to get

  $$\sqrt{N_X} = \sqrt{\frac{E_{\text{dep}} - N_{\text{i}} E_{\text{i}}}{E_X}}.$$

  The fluctuations in N_{i} are then

  $$\sigma_{\text{i}} = \frac{E_X}{E_{\text{i}}}\sigma_X = \frac{E_X}{E_{\text{i}}}\sqrt{\frac{E_{\text{dep}} - N_{\text{i}} E_{\text{i}}}{E_X}}.$$

  We then substitute in $N_{\text{i}} = E_{\text{dep}}/w$ and get

  $$\sigma_{\text{i}} = \frac{E_X}{E_{\text{i}}}\sqrt{\frac{E_{\text{dep}}}{E_X} - \frac{E_{\text{i}}}{E_X}\frac{E_{\text{dep}}}{w}} = \sqrt{\frac{E_{\text{dep}}}{w}}\sqrt{\frac{E_X w}{E_{\text{i}}^2} - \frac{E_X}{E_{\text{i}}}};$$

  a few more steps of algebra produce

  $$\sigma_{N_{\text{i}}} = \sqrt{\frac{E_{\text{dep}}}{w}}\sqrt{\frac{E_X}{E_{\text{i}}}\left(\frac{w}{E_{\text{i}}} - 1\right)} = \sqrt{N_{\text{i}}}\sqrt{\frac{E_X}{E_{\text{i}}}\left(\frac{w}{E_{\text{i}}} - 1\right)} \equiv \sqrt{N_{\text{i}}}F,$$

  where F is dimensionless constant called the *Fano factor*. The Fano factor is real because $w > E_{\text{i}}$. (Note that the above might be $\sqrt{F}$, i.e. the Fano factor is only the argument of the square root $F = \frac{E_X}{E_{\text{i}}}\left(\frac{w}{E_{\text{i}}} - 1\right)$.)

- Finally, using $E_{\text{dep}} = wN_i$, we note that

$$\frac{\sigma_{E_{\text{dep}}}}{E_{\text{dep}}} = \frac{\sigma_{N_{\text{i}}}}{N_{\text{i}}} = \sqrt{\frac{E_{\text{dep}}}{w}F}\frac{w}{E_{\text{dep}}} = \sqrt{\frac{w}{E_{\text{dep}}}F}$$

  The lesson here is that because (quoting from lecture) many detectors have a small Fano factor $F \ll 1$, it is possible for relative energy uncertainty $\frac{\sigma_{E_{\text{dep}}}}{E_{\text{dep}}}$ to be much smaller for a particle fully stopping in a detector than for a particle passing through a detector.

2.4 Transport of Electrons and Ions in Gas

2.4.1 Transport In the Absence of an Electric Field

- In the absence of an external electric field, electrons and ions move as a result of thermal motion. If we model the electrons and ions as classical (and not quantum) particles, their speeds are distributed according a Maxwell-Boltzmann distribution, in which the portion of particles in an infinitesimal element $\mathrm{d}^3\mathbf{v}$ of three-dimensional velocity space centred around a velocity vector of magnitude v is

$$f(v)\,\mathrm{d}^3\mathbf{v} = \left(\frac{m}{2\pi k_B T}\right)^{3/2} e^{-\frac{mv^2}{2k_B T}}\,\mathrm{d}^3\mathbf{v},$$

  where m would be replaced by the electron or ion mass. The corresponding distribution of electron/ion speeds, using $\mathrm{d}^3\mathbf{v} \to 4\pi v^2\,\mathrm{d}v$, is

$$f(v)\,\mathrm{d}v = 4\pi\left(\frac{m}{2\pi k_B T}\right)^{3/2} v^2 e^{-\frac{mv^2}{2k_B T}}\,\mathrm{d}v.$$

  The mean speed of electrons and ions in the gas is thus

$$\langle v\rangle = \int_0^\infty v f(v)\,\mathrm{d}v = \sqrt{\frac{8k_B T}{\pi m}}.$$

  Note that, because $v \sim m^{-1}$, the thermal speeds of electrons ($\sim 10^4\,\mathrm{m\,s^{-1}}$) are much larger than thermal ion speeds ($\sim 10^2\,\mathrm{m\,s^{-1}}$) at typical room temperature and pressure.

- Quoting from kinetic theory, the mean free path ℓ of an electron (ion) with characteristic length L in a gas at pressure p is approximately

$$\ell = \frac{k_B T}{\sqrt{2\pi^2} p L^2}.$$

- Main lesson here: because of random thermal motion, electrons and ions (even in the absence of an external electric field) will spread out in position space from their point of initial creation.

  We only summarize some results from elementary transport theory. The transport of electrons (ions) through the gas is given by the transport equation

$$\mathbf{j}(\mathbf{r}, t) = -D\nabla n(\mathbf{r}, t),$$

  where $n(\mathbf{r}, t)$ is the number density of electrons (ions) at position $\mathbf{r}$ at time t, D is the diffusion constant (SI units $\mathrm{m^2\,s^{-1}}$) and $\mathbf{j}(\mathbf{r}, t)$ is the number current density of electrons (ions) at at position $\mathbf{r}$ at time t.

- Again quoting from kinetic theory, the spread σ in position space of electrons (ions) about their initial position of formation is

$$\sigma(t) = \sqrt{6Dt}, \tag{2.6}$$

and, because of thermal motion, increases with time t. Again without derivation, the diffusion constant may be written in terms of mean speed $\langle v \rangle$ and mean free path ℓ as

$$D = \frac{1}{3} \langle v \rangle \ell \propto \sqrt{\frac{T}{m}} \cdot \frac{T}{p} = \frac{T^{3/2}}{p\sqrt{m}}.$$

Conclusions: in the absence of an electric field, the diffusion of electrons (ions) from their initial positions increases with increasing T and decreasing p. Because $D \propto 1/\sqrt{m}$, electrons spread out more in the gas than ions.

2.4.2 Transport in an Electric Field

In the presence of an electric field (as is the case in gas-based detectors, which have a potential difference applied across the gas) positive ions are accelerated in the direction of the electric field and negative electrons in the direction opposite the electric field.

As ions (electrons) accelerate through the gas, they collide with gas atoms and loose energy. On a *microscopic* scale, the motion of ions (electrons) looks something like: (i) acceleration in direction of electric field; (ii) collision with gas atom, loss of energy; (iii) acceleration in direction of electric field; (iv) collision, loss of energy, and so on...

On a *macroscopic* scale, we model ions (or electrons) as drifting through the gas in the direction of (or opposite of) the electric field with a constant drift velocity v_d proportional to the electric field, i.e.

$$v_\mathrm{d}^{(\mathrm{i})} = \mu_\mathrm{i} E \qquad \text{and} \qquad v_\mathrm{d}^{(\mathrm{e})} = \mu_\mathrm{e} E,$$

where the proportionality constant μ is called ion (or electron) *mobility*. In principle μ is also a function of electric field (in particular for the less massive electrons), but we will assume μ is constant.

Representative Numerical Values

- For orientation, we now quote some representative numerical values. Consider a cylindrical detector with potential difference $U_0 \sim 200\,\mathrm{V}$, a housing/anode wire radius ratio $R/r_0 \sim 200$, housing radius $R = 2\,\mathrm{cm}$ and anode wire radius $r_0 = 0.1\,\mathrm{mm}$. Let $r^* \sim 0.15\,\mathrm{mm}$ be the position near the anode wire where most secondary ionization occur. The electric field in the detector at r^* is

$$E = \frac{U_0}{\ln(R/r_0)} \frac{1}{r^*} \approx 2.5\,\mathrm{kV\,cm^{-1}}.$$

- A tabulated value for argon mobility is $\mu_\mathrm{i} = 1.7\,\mathrm{cm^2\,V^{-1}\,s^{-1}}$; the corresponding argon ion drift speed is then

$$v_\mathrm{d}^{(\mathrm{i})} = \mu_\mathrm{i} E = 1.7\,\mathrm{cm^2\,V^{-1}\,s^{-1}} \cdot 2.5\,\mathrm{kV\,cm^{-1}} \approx 4.3 \cdot 10^3\,\mathrm{cm\,s^{-1}}.$$

Meanwhile, a tabulated mean thermal velocity for argon ions is of the order

$$\langle v_\mathrm{i} \rangle \sim 4 \cdot 10^4\,\mathrm{cm\,s^{-1}} \gg v_\mathrm{d}^{(\mathrm{i})}.$$

- Tabulated electron mobility: (was not given in lecture). We simply quoted the representative drift speed
$$v_{\mathrm{d}}^{(\mathrm{e})} \sim 5 \cdot 10^6 \,\mathrm{cm\,s^{-1}}.$$
Meanwhile, a tabulated mean thermal velocity for electrons in argon at typical temperatures is
$$\langle v_{\mathrm{e}} \rangle \sim 10^7 \,\mathrm{cm\,s^{-1}} \sim v_{\mathrm{d}}^{(\mathrm{e})}.$$

- The key points here are:
  (a) Ion drift speed $v_{\mathrm{d}}^{(\mathrm{i})}$ is considerably less than typical thermal speeds $\langle v_{\mathrm{i}} \rangle$.
  (b) Electron drift speed $v_{\mathrm{d}}^{(\mathrm{e})}$ is of comparable order to thermal speeds $\langle v_{\mathrm{e}} \rangle$.
  (c) Both electron drift and thermal speeds are considerably larger than their ion counterparts (since electrons are considerably lighter).

  The corresponding conclusions are:
  (a) The average position of positive ions does not move considerably from the point of creation, because (i) random thermal motion dominates drift velocity and (ii) ion speeds are relatively small.
  (b) Electrons, meanwhile, have a drift velocity comparable to thermal velocity, and both of these velocities are also much larger than the positive ion velocities.
  (c) Electrons move in the direction opposite electric field (because of a drift speed larger than random thermal speed) with a dispersion much larger than that of the positive ions.

  The net result is that each ion pair creation results in a characteristic teardrop distribution of electric charge in the detector: positive ions are concentrated at the point of secondary ionizations, while electrons spread out in a teardrop shape in the direction opposite the electric field.

2.5 Electric Signal Dynamics

In this section we will analyze the electronic signal produced by an ionization avalanche in a cylindrical gas-based detector in the proportional counting regime.

Consider an incident ionizing particle freeing N_0 primary ions in a cylindrical detector with multiplication factor M. The total number of secondary ion pairs N, after multiplication, is
$$N = MN_0.$$

2.5.1 Voltage Dependence on Position

- For review from Equation 2.1 and 2.2, the electric field and electric potential in a cylindrical detector are
$$\mathbf{E}(\mathbf{r}) = \frac{U_0}{\ln(R/r_0)} \frac{\hat{\mathbf{e}}_r}{r} \qquad \text{and} \qquad \phi(r) = -\frac{U_0}{\ln(R/r_0)} \ln \frac{r}{R}.$$
(The expression for potential assumes $\phi(R) = 0$ and $\phi(r_0) = V_0$.) The electrostatic potential energy of a point charge q in a electric field is
$$W_{\mathrm{E}} = q\phi.$$

- When a charged particle moves a radial distance $\mathrm{d}r$ through the detector's radial electric field, its potential energy changes by

$$\mathrm{d}W_\mathrm{E} = q\frac{\partial\phi}{\partial r}\,\mathrm{d}r = -q\frac{U_0}{\ln(R/r_0)}\frac{\mathrm{d}r}{r}.$$

  We aim to convert this energy change into a change in voltage, which we would detect in experiment. For review from electrostatics, the electric energy stored in a capacitor of capacitance C with potential difference U between the capacitor plates is

$$W_\mathrm{C} = \frac{1}{2}U^2 \implies \mathrm{d}W_\mathrm{C} = CU\,\mathrm{d}U.$$

  For the detector, $U \approx U_0$ throughout the avalanche process—the charge freed by the avalanche is small relative to the charge on the capacitor plates, so the resulting change in voltage is small relative to the steady-state value U_0.

- By conservation of energy, the change in particle electrostatic energy $\mathrm{d}W_\mathrm{E}$ moving through the detector must equal the change in the capacitor's energy $\mathrm{d}W_\mathrm{C}$:

$$\mathrm{d}W_\mathrm{C} = \mathrm{d}W_\mathrm{E} \implies CU_0\,\mathrm{d}U = -\frac{qU_0}{\ln(R/r_0)}\frac{\mathrm{d}r}{r}.$$

  We then rearrange to get

$$\frac{\mathrm{d}U}{\mathrm{d}r} = -\frac{q}{C\ln(R/r_0)}\frac{1}{r}. \tag{2.7}$$

- We first consider an electron, which has charge $q = -e_0$ and moves from the ionization position r^* to the anode wire r_0. The change in voltage on the detector capacitor plates from an electron is thus

$$\Delta U_\mathrm{e} = -\frac{q}{C\ln R/r_0}\int_{r^*}^{r_0}\frac{\mathrm{d}r}{r} = \frac{e_0}{C\ln(R/r_0)}\ln\frac{r_0}{r^*}.$$

  We then consider a positive ion, which has charge $q = +e_0$ and moves from r^* to the outer cathode surface at $r = R$. The change in voltage on the detector capacitor plates from a positive ion is thus

$$\Delta U_\mathrm{i} = -\frac{q}{C\ln R/r_0}\int_{r^*}^{R}\frac{\mathrm{d}r}{r} = -\frac{e_0}{C\ln(R/r_0)}\ln\frac{R}{r^*}.$$

  The total voltage change from both an electron and ion is the sum

$$\begin{aligned}\Delta U = \Delta U_\mathrm{e} + \Delta U_\mathrm{i} &= -\frac{e_0}{C\ln(R/r_0)}\left(\ln\frac{R}{r'} - \ln\frac{r_0}{r'}\right)\\ &= -\frac{e_0}{C\ln(R/r_0)}\ln\frac{R}{r_0}\\ &= -\frac{e_0}{C}.\end{aligned}$$

  Lesson: the voltage drop ΔU is the same as if the change on the capacitor plates changed by one elementary charge.

- Important: it turns out that only positive ions contribute appreciably to the measured detector signal. To confirm this, we consider the ratio

$$\frac{\Delta U_{\mathrm{i}}}{\Delta U_{\mathrm{e}}} = \frac{\ln(R/r^*)}{\ln(r_0/r^*)}.$$

The vast majority of all ions in the detector come from secondary ionizations near the anode wire, so $r^* \sim r_0$ and $R \gg r^*$. This implies

$$\frac{\Delta U_{\mathrm{i}}}{\Delta U_{\mathrm{e}}} = \frac{\ln(R/r^*)}{\ln(r_0/r^*)} \gg 1.$$

Lesson: Positive ions contribute far more to change in voltage than electrons. Physical reason is because ions travel much farther through the detector before reaching a capacitor electrode, resulting in a larger change in ion potential energy and a corresponding large drop in capacitor voltage.

2.5.2 Signal Dynamics

- Equation 2.7 gives the dependence of detector voltage U on the radial position r of charged particles in the detector. We now aim to convert this to dependence of voltage on time using the chain rule:

$$\frac{\mathrm{d}U}{\mathrm{d}t} = \frac{\mathrm{d}U}{\mathrm{d}r}\frac{\mathrm{d}r}{\mathrm{d}t}.$$

We begin with $\frac{\mathrm{d}U}{\mathrm{d}r}$ from Equation 2.7, which for review reads

$$\frac{\mathrm{d}U}{\mathrm{d}r} = -\frac{q}{C\ln(R/r_0)}\frac{1}{r}.$$

We then find $U(t)$ using the chain rule:

$$\begin{aligned} U(t) &= \int_0^{U(t)} \mathrm{d}U = \int_{r(t=0)}^{r(t)} \frac{\mathrm{d}U}{\mathrm{d}r}\,\mathrm{d}r \\ &= -\frac{q}{C\ln(R/r_0)}\int_{r^*}^{r(t)} \frac{\mathrm{d}r}{r} \\ &= -\frac{q}{C\ln(R/r_0)}\ln\frac{r(t)}{r^*}. \end{aligned} \tag{2.8}$$

We have reduced the computation of the voltage dynamics $U(t)$ to computing the electron's trajectory $r(t)$ through the detector.

It remains to find the ion trajectory $r(t)$. We first recall the expression for drift velocity in Equation 2.4.2, i.e.

$$\frac{\mathrm{d}r}{\mathrm{d}t} = v_{\mathrm{d}} = \mu E = \frac{\mu U_0}{\ln(R/r_0)}\frac{1}{r}, \tag{2.9}$$

where μ is either electron or ion mobility. We can use the above expression for $\frac{\mathrm{d}r}{\mathrm{d}t}$ to find $r(t)$ for both positive ions and electrons.

Voltage Signal for Positive Ions

- For positive ions Equation 2.9 reads

$$\frac{\mathrm{d}r}{\mathrm{d}t} = v_{\mathrm{d}}^{(\mathrm{i})} = \frac{\mu_{\mathrm{i}} U_0}{\ln(R/r_0)} \frac{1}{r}.$$

We rearrange and integrate from $r(0) = r^* \approx r_0$ to arbitrary $r(t)$, giving

$$\int_{r_0}^{r(t)} r \, \mathrm{d}r = \frac{\mu_{\mathrm{i}} U_0}{\ln(R/r_0)} \int_0^t \mathrm{d}t.$$

We then carry out the integration to get

$$r^2(t) - r_0^2 = \frac{2\mu_{\mathrm{i}} U_0}{\ln(R/r_0)} t,$$

then solve for $r(t)$ to get

$$r_{\mathrm{i}}(t) = \sqrt{\frac{2\mu_{\mathrm{i}} U_0}{\ln(R/r_0)} t + r_0^2} \equiv r_0 \sqrt{1 + t/t_0^+}, \tag{2.10}$$

where we have defined the characteristic positive ion travel time as

$$t_0^+ \equiv \frac{r_0^2 \ln(R/r_0)}{2\mu_{\mathrm{i}} U_0}.$$

Ions reach the cathode at the time t_{i} solving the equation $r_{\mathrm{i}}(t_{\mathrm{i}}) = R$. This is

$$R = r_0 \sqrt{1 + t_{\mathrm{i}}/t_0^+} \implies t_{\mathrm{i}} = \left(\frac{R^2}{r_0^2} - 1 \right) \cdot t_0^+$$

- We then return to Equation 2.8 for $U(t)$, make the approximation $r^* \approx r_0$, and substitute in the just-derived $r(t)$ to get the voltage signal resulting from the motion of positive ions through the detector:

$$\begin{aligned} U_{\mathrm{i}}(t) &\approx -\frac{q}{C \ln(R/r_0)} \ln \frac{r_{\mathrm{i}}(t)}{r_0} = -\frac{e_0}{C \ln(R/r_0)} \ln \left[\frac{1}{r_0} \left(r_0 \sqrt{1 + \frac{t}{t_0^+}} \right) \right] \\ &= -\frac{e_0}{2C \ln(R/r_0)} \ln \left(1 + \frac{t}{t_0^+} \right), \end{aligned}$$

where we have used $q = e_0$ for a positive ion and the logarithm property $\ln a^b = b \ln a$ to simplify the square root in the logarithm.

Voltage Signal for Electrons

- The velocity of electrons through the detector (electrons move radially inward, in the direction of decreasing r) is

$$\frac{\mathrm{d}r}{\mathrm{d}t} = v_{\mathrm{d}}^{(\mathrm{e})} = -\mu_{\mathrm{e}} E = -\frac{\mu_{\mathrm{e}} U_0}{\ln(R/r_0)} \frac{1}{r}.$$

We then find $r(t)$ by rearranging differentials and integrating

$$\int_{r^*}^{r(t)} r \, \mathrm{d}r = -\frac{\mu_{\mathrm{e}} U_0}{\ln(R/r_0)} \int_0^t \mathrm{d}t.$$

We cannot set the initial ionization position $r(0) = r^* = r_0$, since the final r—when electrons reach anode wire—is also r_0. Instead we adopt the ion result in Equation 2.10 and write

$$r_\mathrm{e}(t) = r^*\sqrt{1 - t/t_0^-}, \quad \text{where } t_0^- \equiv \frac{(r^*)^2 \ln(R/r_0)}{2\mu_\mathrm{e} U_0}.$$

Keep in mind that electrons travel up to $r(t) \geq r_0$ (i.e. electrons to not penetrate into the anode wire). Electrons reach the anode wire at the time t_e solving the equation $r_\mathrm{e}(t_\mathrm{e}) = r_0$. This is

$$r_0 = r^*\sqrt{1 - t_\mathrm{e}/t_0^-} \implies t_\mathrm{e} = \left[1 - \frac{r_0^2}{(r^*)^2}\right] \cdot t_0^-.$$

(Note that t_e is positive only so long as $r^* > r_0$, i.e. as long as ionizations occur at radial positions larger than the radius of the anode wire, which makes physical sense.) We then substitute $r(t)$ into Equation 2.8 for $U(t)$ and again make the approximation $r^* \approx r_0$ to get the voltage signal resulting from the motion of electrons through the detector:

$$\begin{aligned} U_\mathrm{e}(t) &\approx -\frac{q}{C\ln(R/r_0)} \ln\frac{r_\mathrm{e}(t)}{r_0} = +\frac{e_0}{C\ln(R/r_0)} \ln\left[\frac{1}{r_0}\left(r_0\sqrt{1 - \frac{t}{t_0^-}}\right)\right] \\ &= \frac{e_0}{2C\ln(R/r_0)} \ln\left(1 - \frac{t}{t_0^-}\right), \end{aligned}$$

where we have used $q = -e_0$ for a negative electron and the logarithm property $\ln a^b = b \ln a$ to simplify the square root in the logarithm. Note that the logarithm's argument becomes negative for $t > t_\mathrm{e}$, so $U_\mathrm{e}(t)$ is defined only for $t < t_\mathrm{e}$.

- For orientation: consider a detector with the parameters $r_0 = 0.1\,\mathrm{mm}$ and $R/r_0 = 200$ and $U_0 = 200\,\mathrm{V}$, and assume charge carrier mobilities $\mu_+ = 1.7\,\mathrm{cm^2\,V^{-1}\,s^{-1}}$ and $\mu_- = 2 \cdot 10^3\,\mathrm{cm^2\,V^{-1}\,s^{-1}}$. In this case the values of t_0^+ and t_0^- come out to $t_0^+ \sim 1\,\mu\mathrm{s}$ and $t_0^- \sim 0.002 \cdot t_0^+$.

2.6 Position-Sensitive Detectors

- Position-sensitive detectors measure the position at which an ionizing particle passed through a detector (while the detectors we have described so far could only register that a particle passed *somewhere* through a detector, but could did not give information about the position within the detector).
- Aside from giving useful position information in their own right, position-sensitive detectors are critical to measuring the momenta of charged particles. Specifically, a charged particle's curvature in an external magnetic field under the influence of the Lorentz force $\mathbf{F} = q\mathbf{v} \times \mathbf{B}$ is proportional to the particle's momentum. Thus, if a particle's trajectory (i.e. a sequence of position measurements) in a magnetic field is known, the particle momentum can be reconstructed from the trajectory's curvature.
- In the following sections, we briefly outline with working principles of common position-sensitive detectors.

2.6.1 Multi-Wire Proportional Chamber

- A multi-wire proportional chamber (MWPC) is a rectangular gas-filled chamber. The chamber's upper and lower plates serve as cathodes and are typically grounded, while

wires running through the chamber parallel to the upper and lower plate serve as anodes and are held at positive potential $+U_0$. Each anode wire has an independent electronic read-out system. Quoting from lecture, a typical separation between the upper and lower plates is about 10 mm while wire spacing is roughly 1 to 2 mm.

The electric field in the chamber is approximately homogeneous near the plate surfaces and approximately radial near the anode wires.

- A MWPC's working principle:

  1. An incident particle ionizes the gas in the chamber, and the primary ions are accelerated in the (approximately) uniform electric field between plates.
  2. Upon approaching and anode wire, where the electric field becomes locally radial and scales as $E \sim 1/r$, the primary electrons cause an avalanche of secondary ionizations.
  3. The secondary electrons produce a measurable electric signal on the anode wire. Because the primary electrons are mostly likely to reach the anode wire closest to the position of primary ionization, the wire outputting the strongest signal encodes the likely position of the initial incident particle.

  Note that positive ions accelerate to the cathode plates and also give a secondary, but weaker signal than anode wire electrons.

- The uniform electric field far from the anode wires is important for preserving spatial information about the initial ionizing particle—hence the choice of planar geometry. The goal is for particles to move directly "downward" (i.e. normal to the upper and lower plates) to the wire immediately below the point of ion creation. This preserves information about initial particle's incident position.

- Note that the above-described configuration measures only a single coordinate of incident particle position in detector. The detector measures the anode wire at which secondary ionizations occurred, but not the position along the wire, i.e. the coordinate parallel to the anode wires.

  In practice, the cathode plates are segmented into strips oriented perpendicular to the anode wires. Positive ions reaching cathode strips then measure the second coordinate in the plane of the cathode plates which is not measured by anode wires. (The vertical position of the primary ionization between the cathode plates remains unknown.)

Resolution

- We now consider the distribution of an incident particle's position between two anode wires separated by a distance a. We place the origin between the wires, so that the wires occur at $x = \pm a/2$.

- Assume we consider only the strongest signal from the primary anode. Because of translational symmetry in the planar direction perpendicular to the wires, if we take only the strongest wire signal we may assume incident particles only fall between the two wires and nowhere else. Incident particle position is uniformly distributed between the wires:

$$\frac{\mathrm{d}P}{\mathrm{d}x} = \frac{1}{a} \begin{cases} 1 & -\frac{a}{2} \leq x < \frac{a}{2} \\ 0 & \text{otherwise.} \end{cases}$$

The expected value $\langle x \rangle$ of incident particle position is

$$\langle x \rangle = \int_{-a/2}^{a/2} x \frac{\mathrm{d}P}{\mathrm{d}x} \, \mathrm{d}x = 0,$$

while the expected value $\langle x^2 \rangle$ of position squared is

$$\langle x^2 \rangle = \int_{-a/2}^{a/2} x^2 \frac{\mathrm{d}P}{\mathrm{d}x} \, \mathrm{d}x = \frac{a^2}{12}.$$

The spatial resolution for this simple model is thus

$$\sigma_x^2 = \langle x^2 \rangle - \langle x \rangle^2 = \frac{a^2}{12} \implies \sigma_x = \frac{a}{\sqrt{12}}.$$

As might be expected, position resolution improves (decreases) as the wires grow closer together.

- A better result comes from considering signals from multiple anodes—we will consider measuring particle position by taking the positions of the two wires with the strongest and second-strongest signals. Let r denote the ratio of signal strengths on each wire. The distribution of particle position x is then

$$\frac{\mathrm{d}P}{\mathrm{d}x} = \frac{2}{a} \begin{cases} r & -\frac{a}{2} \leq x < 0 \\ (1-r) & 0 \leq x < \frac{a}{2} \\ 0 & \text{otherwise,} \end{cases}$$

where the coefficient $2/a$ ensures the distribution is properly normalized. The expected value of position is

$$\langle x \rangle = \frac{2}{a} \left[\int_{-a/2}^{0} rx \, \mathrm{d}x + \int_{0}^{a/2} (1-r)x \, \mathrm{d}x \right] = \frac{a}{4} \cdot (1-2r).$$

The corresponding value of $\langle x^2 \rangle$ is

$$\langle x^2 \rangle = \frac{2}{a} \left[\int_{-a/2}^{0} rx^2 \, \mathrm{d}x + \int_{0}^{a/2} (1-r)x^2 \, \mathrm{d}x \right] = \frac{a^2}{12}.$$

The position resolution for two wires thus improves to

$$\sigma_x^2 = \langle x^2 \rangle - \langle x \rangle^2 = \frac{a^2}{12} \left[1 - \frac{3}{4}(1-2r)^2 \right].$$

The quantity in square brackets is less than or equal to one for all r, so the two-wire resolution is better than the single-wire result $\sigma_x^2 = a^2/12$.

- Quoting from lecture, the resolution of position measurements in a typically MWPC is of the order $\sigma_x \sim 100\,\mu\mathrm{m}$.

Wire Sagging

- The anode wires used in gas-based detectors sag under their own weight. This is undesirable, since the electric field from a sagging wire deviates from the predictable, purely radial field associated with a perfectly straight wire.

  We will now briefly analyze the mechanics of wire sag. Consider a two-dimensional problem in which a wire of density ρ and cross section S held taught with tension force T runs along the x axis and sags along the y.

  We then consider an infinitesimal segment of length $\mathrm{d}x$; the tension at the segment's endpoints are $T(x)$ and $T(x+\mathrm{d}x)$, while the segment's weight is

  $$F_\mathrm{g} = g\rho\,\mathrm{d}V = g\rho S\,\mathrm{d}x.$$

  Let ϕ denote the (small) angle between the wire and the x axis, so that $y' = \frac{\mathrm{d}y}{\mathrm{d}x} = \tan\phi$. The tension component in the y direction at the x coordinate $x+\mathrm{d}x$ is

  $$T_y(x+\mathrm{d}x) = T(x+\mathrm{d}x)\sin\phi \approx T(x+\mathrm{d}x)\tan\phi = T(x+\mathrm{d}x)\cdot y'(x+\mathrm{d}x).$$

  Similarly

  $$T_y(x) = T(x)\cdot y'(x).$$

  We then assume $T(x) \approx T(x+\mathrm{d}x) \equiv T$ and equate the segment's weight to the difference in y tension components at the segment ends

  $$\rho S g\,\mathrm{d}x = T_y(x+\mathrm{d}x) - T_y(x) = T\cdot\left[y'(x+\mathrm{d}x) - y'(x)\right]$$

  We then divide through by $\mathrm{d}x$ and recognize the difference quotient:

  $$\rho S g = T\cdot\frac{y'(x+\mathrm{d}x)-y'(x)}{\mathrm{d}x} = Ty''.$$

  We then rearrange to get an equation for the sagging profile $y(x)$:

  $$y'' = \frac{\mathrm{d}^2y}{\mathrm{d}x^2} = \frac{\rho S g}{T} \implies y(x) = \frac{\rho S g}{2T}x^2 + Ax + B.$$

  We determine the integration constants from the boundary conditions $y(\pm L/2) = 0$ (i.e. the wire is fixed at its endpoints), which give $A = 0$ and $B = \rho g S L^2/(8T)$. The complete solution for the wire's profile is then

  $$y(x) = \frac{\rho S g}{2T}\left[x^2 - \frac{L^2}{4}\right].$$

  The greatest displacement occurs at the midpoint at $x = 0$ and equals

  $$y_\mathrm{max} = -\frac{\rho S g L^2}{8T}.$$

  Sagging is evidently minimized by larger tension T and shorter, narrower, and denser wires. Of course, we cannot increase wire tension (and thus minimize sagging) indefinitely—at some critical tension T_crit the wires snap. Anode wires are often made of wolfram, which has relatively large T_crit and allows high wire tensions, and thus relatively small sagging.

2.6.2 Drift Chamber

- A drift chamber consists of a cylindrical detector, field wire region, and cathode, all enclosed in a roughly tube-like outer housing. On one side of tube is a cathode held at negative potential, e.g. $-|U_0|$. On the other side of the outer housing is a gas-filled cylindrical detector working in the proportional counting regime described in Section 2.1. This counter has a central anode wire at $+U_0$ and a grounded cathode housing, and a slit so that particles can enter the cylindrical detector.

  Between the anode and cathode are uniformly spaced field lines (parallel to anode wire) used to establish a desired electric field distribution in the region between anode and cathode. Because of the slit in the cylindrical gas-based detector, the gas from the cylindrical detector thus fills entire field wire region.

- Working principle:

  1. An ionizing particle incident on field wire region produces *primary* electrons.
  2. The field wires are designed so that these primary electrons drift at constant (assumed-to-be-known) drift velocity v_d into the cylindrical counter's opening.
  3. Upon reaching the cylindrical counter's anode wire, the primary electrons cause a measurable ion avalanche.

- To analyze the drift chamber, define a coordinate x in the direction from the cylindrical detector to the $-|U_0|$ cathode.

  Our goal is to identify x position of incident ionizing particle. To do this, in practice one places a scintillator detector on the outer housing of drift chamber. Scintillation detectors, discussed more in Section 4 are fast and used in this case to determine the time t_0 when the initial ionizing particle entered the drift chamber.

  We determine x from the time taken by primary electrons to travel along x axis from position of primary ionization to anode wire via the simple relationship

  $$x = \int_{t_0}^{t_1} v_\mathrm{d}\,\mathrm{d}t,$$

  where t_0 is scintillator signal time, and t_1 is the time when signal appears in the cylindrical proportional counter—the anode. We estimate v_d from $v_\mathrm{d} = \mu_\mathrm{e} E$, so we must know both the mobility and electric field in the detector chamber.

- The spatial resolution of the x measurement is limited by (random) thermal diffusion of ions and electrons. Using the expression for position fluctuation $\sigma(t)$ from Equation 2.6 and expressing the time t for an ion in a drift chamber to travel from its initial position to x via $t = x/v_\mathrm{d}$, the resolution in a drift chamber position measurement is of the order

  $$\sigma_x = \sqrt{6Dt} = \sqrt{6D\frac{x}{v_\mathrm{d}}} = \sqrt{6D\frac{x}{\mu_\mathrm{e}E}},$$

  where D is the diffusion constant and t is the drift time from initial primary electron creation point to the point of detection x.

  Because uncertainty increases with x, we aim to keep x small. Typical values of x for distance of particle drift across the chamber are of the order $x \sim 5\,\mathrm{cm}$. Typical spatial resolutions in drift chambers are of the order $\sigma_x \lesssim 100\,\mu\mathrm{m}$, like for good MWPC.

3 Semiconductor Detectors

I assume the reader is familiar with basic semiconductor physics from Solid State Physics, so I am leaving out a review of semiconductors in these notes.

3.1 Diffused-Junction Diode

A diffused-junction diode is essentially the p-n junction diode familiar from foundational semiconductor physics; the name diffused-junction diode just refers to the manufacturing process in which a gas of donor dopants is diffused into a p-type semiconductor to form a p-n junction.

3.1.1 Depletion Region Width

- Our goal in this section is to determine the width of the depletion region in a p-n junction.

  Assume the initial (pre-depletion region creation) boundary between the p-type and n-type semiconductor is well-defined and occurs at $x = 0$. Assume the p-type and n-type sides of the depletion region span $x \in (-x_\mathrm{p}, 0)$ and $x \in (0, x_\mathrm{n})$, respectively.

  Let N_a and N_d denote the concentrations of acceptor dopants in the p-type region and of donor dopants in the n-type region, respectively. For simplicity, we assume the charge density ρ in the depletion region is a step function of the form

$$\rho(x) = \begin{cases} -e_0 N_\mathrm{a} & x \in (-x_\mathrm{p}, 0) \\ e_0 N_\mathrm{d} & x \in (0, x_\mathrm{n}), \end{cases} \tag{3.1}$$

  where the entire depletion region spans the x range $(-x_\mathrm{p}, x_\mathrm{n})$. We begin our analysis with the Poisson equation from electrostatics, which reads

$$\nabla^2 \phi(\mathbf{r}) = -\frac{\rho(\mathbf{r})}{\epsilon\epsilon_0},$$

  and in a one-dimensional case reduces to

$$\frac{\mathrm{d}^2\phi}{\mathrm{d}x^2} = -\frac{\rho(x)}{\epsilon\epsilon_0} \implies \frac{\mathrm{d}\phi}{\mathrm{d}x} = -\int \frac{\rho(x)}{\epsilon\epsilon_0}\,\mathrm{d}x.$$

  We then integrate the charge density in Equation 3.1 from $-x_\mathrm{p}$ to x_n to get

$$\frac{\mathrm{d}\phi}{\mathrm{d}x} = \begin{cases} \frac{e_0 N_\mathrm{a}}{\epsilon\epsilon_0} x + c_\mathrm{p} & x \in (-x_\mathrm{p}, 0) \\ -\frac{e_0 N_\mathrm{d}}{\epsilon\epsilon_0} x + c_\mathrm{n} & x \in (0, x_\mathrm{n}). \end{cases}$$

  As boundary conditions we require $\frac{\mathrm{d}\phi}{\mathrm{d}x} = 0$ (i.e. zero electric field) at the depletion region boundaries $x = x_\mathrm{n}$ and $x = -x_\mathrm{p}$. This condition produces

$$\frac{\mathrm{d}\phi}{\mathrm{d}x} = \begin{cases} \frac{e_0 N_\mathrm{a}}{\epsilon\epsilon_0}(x + x_\mathrm{p}) & x \in (-x_\mathrm{p}, 0) \\ -\frac{e_0 N_\mathrm{d}}{\epsilon\epsilon_0}(x - x_\mathrm{n}) & x \in (0, x_\mathrm{n}). \end{cases} \tag{3.2}$$

  We then integrate over x once more to get the depletion region potential

$$\phi(x) = \begin{cases} \frac{e_0 N_\mathrm{a}}{\epsilon\epsilon_0}\left(\frac{x^2}{2} + x_\mathrm{p} x\right) + c_\mathrm{p} & x \in (-x_\mathrm{p}, 0) \\ -\frac{e_0 N_\mathrm{d}}{\epsilon\epsilon_0}\left(\frac{x^2}{2} - x_\mathrm{n} x\right) + c_\mathrm{n} & x \in (0, x_\mathrm{n}), \end{cases}$$

where c_p and c_n are integration constants to be found from boundary conditions.

As a first boundary condition we require continuity of electric potential $\phi(x)$ at the p-n boundary $x = 0$, which produces

$$c_\mathrm{p} = c_\mathrm{n} \equiv c.$$

As a second boundary condition we impose $\phi(-x_\mathrm{p}) = 0$ and $\phi(x_\mathrm{n}) - \phi(-x_\mathrm{p}) = V_0$, (where V_0 is the potential difference across the depletion region). The second boundary conditions leads to

$$\phi(x_\mathrm{n}) = V_0 = \frac{e_0 N_\mathrm{d}}{2\epsilon\epsilon_0} x_\mathrm{n}^2 + c \qquad \text{and} \qquad \phi(-x_\mathrm{p}) = 0 = \frac{-e_0 N_\mathrm{a}}{2\epsilon\epsilon_0} x_\mathrm{p}^2 + c,$$

which we then solve for the integration constant c to get

$$c = \frac{e_0 N_\mathrm{a}}{2\epsilon\epsilon_0} x_\mathrm{p}^2.$$

Substituting c into $\phi(x_\mathrm{n})$ leads to

$$\phi(x_\mathrm{n}) = V_0 = \frac{e_0 N_\mathrm{d}}{2\epsilon\epsilon_0} x_\mathrm{n}^2 + \frac{e_0 N_\mathrm{a}}{2\epsilon\epsilon_0} x_\mathrm{p}^2 = \frac{e_0}{2\epsilon\epsilon_0} \left(N_\mathrm{d} x_\mathrm{n}^2 + N_\mathrm{a} x_\mathrm{p}^2 \right). \tag{3.3}$$

With $c_\mathrm{n} = c_\mathrm{p} \equiv c$ and V_0 known, the depletion region potential comes out to

$$\phi(x) = \begin{cases} \frac{e_0 N_\mathrm{a}}{2\epsilon\epsilon_0}(x + x_\mathrm{p})^2 & x \in (-x_\mathrm{p}, 0) \\ V_0 - \frac{e_0 N_\mathrm{d}}{2\epsilon\epsilon_0}(x - x_\mathrm{n})^2 & x \in (0, x_\mathrm{n}) \end{cases}$$

- Finally, we recall the p-n junction conservation of charge condition

$$N_\mathrm{a} x_\mathrm{p} = N_\mathrm{d} x_\mathrm{n},$$

which we combine Equation 3.3 to solve for x_n and x_p. The result is

$$x_\mathrm{n} = \sqrt{\frac{2\epsilon\epsilon_0 V_0}{e_0 N_\mathrm{d} \left(1 + \frac{N_\mathrm{d}}{N_\mathrm{a}}\right)}} \qquad \text{and} \qquad x_\mathrm{p} = \sqrt{\frac{2\epsilon\epsilon_0 V_0}{e_0 N_\mathrm{a} \left(1 + \frac{N_\mathrm{a}}{N_\mathrm{d}}\right)}}.$$

The total depletion region width d_pn is then

$$d_\mathrm{pn} = x_\mathrm{n} + x_\mathrm{p} = \sqrt{\frac{2\epsilon\epsilon_0 V_0}{e_0} \frac{N_\mathrm{a} + N_\mathrm{d}}{N_\mathrm{a} N_\mathrm{d}}}. \tag{3.4}$$

- Note that if $N_\mathrm{a} \gg N_\mathrm{d}$ then $x_\mathrm{n} \gg x_\mathrm{p}$ and thus $d_\mathrm{pn} \approx x_\mathrm{n}$ which is

$$d_\mathrm{pn} \approx x_\mathrm{n} \approx \sqrt{\frac{2\epsilon\epsilon_0 V_0}{e_0 N_\mathrm{d}}} \qquad (\text{if } N_\mathrm{a} \gg N_\mathrm{d}). \tag{3.5}$$

Analogously, if $N_\mathrm{d} \gg N_\mathrm{a}$ then $x_\mathrm{p} \gg x_\mathrm{n}$ and thus $d_\mathrm{pn} \approx x_\mathrm{p}$ which is

$$d_\mathrm{pn} \approx x_\mathrm{p} \approx \sqrt{\frac{2\epsilon\epsilon_0 V_0}{e_0 N_\mathrm{a}}} \qquad (\text{if } N_\mathrm{d} \gg N_\mathrm{a}). \tag{3.6}$$

- For orientation: Typical number densities of intrinsic atoms (i.e. not dopants, but the intrinsic silicon or germanium from which the doped semiconductor are made) are of the order $5 \cdot 10^{22}\,\mathrm{cm}^{-3}$ atoms in semiconductors
- Typical dopant densities fall in the range $N_\mathrm{a}, N_\mathrm{d} \sim 10^{13}$ to $10^{18}\,\mathrm{cm}^{-3}$, dielectric constants for silicon and germanium semiconductors are of the order $\epsilon \sim 10$ to 15, while typical contact voltages are of the order $V_0 \sim 1\,\mathrm{V}$.

  Typical depletion region widths are of the order $d_\mathrm{pn} \sim 100\,\mu\mathrm{m}$. This is too small to be practical for detection of ionizing in the depletion region.

Increasing Depletion Region Width

- We can increase the width of a depletion region by applying an external *bias* voltage V_b in the reverse bias direction. Typically V_b is of the order of 100 V (perhaps up to 300 V) which increases the depletion region width to $d_\mathrm{pn} \sim 1$ to 5 mm.

  Practical values of V_b are bounded above to about 300 V because of increasing leakage current (causing electrical noise) and risk of dielectric breakdown at high voltage.
- In the presence of reverse biasing, the depletion region width increases to

$$d_\mathrm{pn} = d_0 \sqrt{1 + \frac{V_\mathrm{b}}{V_0}},$$

  where d_0 is the width without biasing (given in Equation 3.4).

Miscellaneous Remarks

- Average energy required for creating an electron-hole pair in a semiconductor detector is of the order $w_\mathrm{sc} \sim 3\,\mathrm{eV}$. This is much smaller than in gas, where ion creation energies are closer to $w_\mathrm{gas} \sim 30\,\mathrm{eV}$.

  Here is a heuristic explanation of smaller w in semiconductors: semiconductors are solid state matter, and thus much denser than gas. An incident particle interacts more strongly with solid state because the constituent atoms are denser, leading to a smaller electron-hole creation energy than the ion creation energy in sparse gases. (Alternatively, more electron-hole pairs are created in semiconductor at a given incident particle energy because of stronger interactions).
- Quoting from lecture, only about a third of an incident particle's energy is used for electron-hole pair production, while the remaining energy goes towards e.g. phonon oscillations of the crystal lattice (which heat the crystal).
- The potential energy jump across a depletion region in a reverse-biased p-n junction is $e_0 V_\mathrm{b} \sim 100\,\mathrm{eV}$ for a 100 V reverse-bias voltage.

  This energy jump far exceeds typical thermal energies (e.g. $k_B T \sim 0.025\,\mathrm{eV}$ at room temperature $T = 300\,\mathrm{K}$), so very few charge carriers pass across the depletion region in the direction opposite majority charge carrier flow.

  But in practice there is a small *leakage current* across any p-n junction. Contributions to the leakage current include:

  – Minority charge carriers (holes in n-type and electrons in p-type). Contribution to current density is nano amperes per squared cm.

- Thermally excited majority charge carriers. This contribution is micro amperes per squared cm.
- "Surface currents" arising from the surface chemistry/preparation of the dopants in the semiconductors. This is largest contribution and is also most difficult to estimate.

3.1.2 Signal Dynamics in Semiconductor p-n Junction

In this section we will derive the charge and current signals resulting from the creation of an electron-hole pair in the depletion region of a p-n junction.

- We begin with an analogous analysis of energy as in Section 2.5.1: the electrostatic potential energy of a point charge q in an electric potential ϕ is

$$W_{\mathrm{E}} = q\phi.$$

When moving a displacement $\mathrm{d}\mathbf{r}$ in the potential, the particle's energy changes by

$$\mathrm{d}W_{\mathrm{E}} = q\nabla\phi \cdot \mathrm{d}\mathbf{r} = -q\mathbf{E} \cdot \mathrm{d}\mathbf{r}.$$

In the semiconductor depletion region $\mathbf{E} = E(x)\,\hat{\mathbf{e}}_x$ and so

$$\mathrm{d}W_{\mathrm{E}} = -qE(x)\,\mathrm{d}x = +q\frac{\partial\phi}{\partial x}\,\mathrm{d}x.$$

- We model the depletion region as a parallel-plate capacitor. The electric energy stored in a capacitor of capacitance C with potential difference U between the capacitor plates is

$$W_{\mathrm{C}} = \frac{1}{2}U^2,$$

and the corresponding change in capacitor energy in response to changing voltage on the capacitor plates is

$$\mathrm{d}W_{\mathrm{C}} = CU\,\mathrm{d}U.$$

As for cylindrical gas-based detector, $U \approx U_0$. We then use the capacitor relationship $Q = CU \implies \mathrm{d}Q = C\,\mathrm{d}U$ to rewrite $\mathrm{d}W_{\mathrm{C}}$ as

$$\mathrm{d}W_{\mathrm{C}} = CU\,\mathrm{d}U = U\,\mathrm{d}Q \approx U_0\,\mathrm{d}Q.$$

- We then equate the energy change $\mathrm{d}W_{\mathrm{E}}$ of an electron or hole moving through the depletion region's electric field to the resulting capacitor energy change $\mathrm{d}W_{\mathrm{C}}$ due to the corresponding redistribution of charge on the capacitor electrodes. This gives

$$\mathrm{d}W_{\mathrm{E}} = \mathrm{d}W_{\mathrm{C}} \implies q\frac{\partial\phi}{\partial x}\,\mathrm{d}x = U_0\,\mathrm{d}Q,$$

where Q is the charge on the capacitor electrodes. We then divide by $\mathrm{d}t$ to get

$$U_0\frac{\mathrm{d}Q}{\mathrm{d}t} = q\frac{\partial\phi}{\partial x}\frac{\mathrm{d}x}{\mathrm{d}t}.$$

Finally, we make the approximation $\frac{\partial\phi}{\partial x} \approx U_0/d_{\mathrm{pn}}$ to get

$$\frac{\mathrm{d}Q}{\mathrm{d}t} = \frac{q}{d_{\mathrm{pn}}}\frac{\mathrm{d}x}{\mathrm{d}t}.$$

Expression for Electric Field

- We estimate electron and hole speeds across the diode junction from the drift velocity relationship
$$\frac{\mathrm{d}x}{\mathrm{d}t} = v_\mathrm{d} = \mu E,$$
where μ is charge carrier mobility and E is the electric field in the depletion region.

- For an easier analysis, we shift the coordinate system so that $x_\mathrm{p} = 0$ and assume the n-type and p-type semiconductors forming the p-n junction are doped such that $N_\mathrm{d} \gg N_\mathrm{a}$. Then
$$E = -\frac{\mathrm{d}\phi}{\mathrm{d}x} = -\frac{e_0 N_\mathrm{a}}{\epsilon\epsilon_0} x.$$
The electrical resistivities in n- and p-type semiconductors are
$$\rho_\mathrm{n} = \frac{1}{e_0 N_\mathrm{d} \mu_\mathrm{e}} \qquad \text{and} \qquad \rho_\mathrm{p} = \frac{1}{e_0 N_\mathrm{a} \mu_\mathrm{h}}.$$

- The p-n junction in our problem (assuming $N_\mathrm{d} \gg N_\mathrm{a}$) consists of two regions: a large p-type region and a small n-type region. We model holes in the p-type region with the time constant
$$\tau_\mathrm{h} \equiv \frac{\epsilon\epsilon_0}{\sigma_\mathrm{E}^{(\mathrm{p})}} = \rho_\mathrm{p} \epsilon\epsilon_0 = \frac{\epsilon\epsilon_0}{e_0 N_\mathrm{a} \mu_\mathrm{h}}.$$
In terms of τ_h, the electric field reads
$$E = -\frac{x}{\mu_\mathrm{h} \tau_\mathrm{h}}. \tag{3.7}$$
For orientation, typical values of τ_h are of the order $\tau \sim 10^{-10}$ to 10^{-11} s. This is much faster than the microsecond-order time constants involved in the signal dynamics of gas-based detectors.

Finding Electron Current

- Using Equation 3.7, the electron speed through the depletion region is
$$\frac{\mathrm{d}x}{\mathrm{d}t} = v_\mathrm{d} = -\mu_\mathrm{e} E = -\mu_\mathrm{e} \cdot \left(-\frac{x}{\mu_\mathrm{h} \tau_\mathrm{h}} \right) = \frac{\mu_\mathrm{e}}{\mu_\mathrm{h}} \frac{x}{\tau_\mathrm{h}}$$
We then separate variables and integrate to find the electron path $x(t)$ through the depletion region. This reads
$$\int_{x_0}^{x(t)} \frac{\mathrm{d}x'}{x'} = \frac{\mu_\mathrm{e}}{\mu_\mathrm{h}} \int_0^t \frac{\mathrm{d}t'}{\tau_\mathrm{h}} \implies x(t) = x_0 e^{\frac{\mu_\mathrm{e}}{\mu_\mathrm{h}} \frac{t}{\tau_\mathrm{h}}}. \qquad \left(\text{for } x \in [0, d_\mathrm{pn}]\right)$$
Of course, this expression only applies in the depletion region; an is no longer valid when an electron reaches the n-type electrode at $x = d_\mathrm{pn}$. We then find the time t_e required for electron to reach the n-type electrode by setting $x = d_\mathrm{pn}$. The result is
$$t_\mathrm{e} = \tau_\mathrm{h} \frac{\mu_\mathrm{h}}{\mu_\mathrm{e}} \cdot \ln \frac{d_\mathrm{pn}}{x_0}.$$
With $x(t)$ known we can compute the total charge accumulated on the semiconductor's n-type electrode; this is
$$Q_\mathrm{e}(t) = -\frac{e_0}{d_\mathrm{pn}} \int_0^t \frac{\mathrm{d}x}{\mathrm{d}t'} \mathrm{d}t' = +\frac{e_0}{d_\mathrm{pn}} x_0 \left(1 - e^{\frac{\mu_\mathrm{e}}{\mu_\mathrm{h}} \frac{t}{\tau_\mathrm{h}}} \right), \qquad (\text{for } t < t_\mathrm{e}). \tag{3.8}$$

where we have used the minus sign to switch the limits of integration. The corresponding electron current is

$$I_{\mathrm{e}}(t) = \frac{\mathrm{d}Q_{\mathrm{e}}}{\mathrm{d}t} = -\frac{e_0}{d_{\mathrm{pn}}}\frac{x_0}{\tau_{\mathrm{h}}}\frac{\mu_{\mathrm{e}}}{\mu_{\mathrm{h}}}e^{\frac{\mu_{\mathrm{e}}}{\mu_{\mathrm{h}}}\frac{t}{\tau_{\mathrm{h}}}}. \qquad \text{(for } t < t_{\mathrm{e}}\text{).} \tag{3.9}$$

Finding Hole Current

- Again using Equation 3.7 to estimate electric field, the hole speed through the depletion region is

$$\frac{\mathrm{d}x}{\mathrm{d}t} = v_{\mathrm{h}} = \mu_{\mathrm{h}}E = \mu_{\mathrm{h}} \cdot \left(-\frac{x}{\mu_{\mathrm{h}}\tau_{\mathrm{h}}}\right) = -\frac{x}{\tau_{\mathrm{h}}}.$$

  As for electrons, we separate variable and solve for the hole path $x(t)$ to get

$$\int_{x_0}^{x(t)} \frac{\mathrm{d}x'}{x'} = -\int_0^t \frac{\mathrm{d}t'}{\tau_{\mathrm{h}}} \implies x(t) = x_0 e^{-\frac{t}{\tau_{\mathrm{h}}}}.$$

  Note that our simple electric field model predicts holes never actually reach the p region, but only approach asymptotically close (because $E \to 0$ as $x \to 0$?).

- Using the hole's time-dependent path $x(t)$, the total charge accumulated on the semiconductor's p-type electrode from holes is then

$$Q_{\mathrm{h}}(t) = +\frac{e_0}{d_{\mathrm{pn}}}\int_0^t \frac{\mathrm{d}x}{\mathrm{d}t'}\,\mathrm{d}t' = -\frac{e_0}{d_{\mathrm{pn}}}x_0\left(1 - e^{-t/\tau_{\mathrm{h}}}\right).$$

  The corresponding hole current is

$$I_{\mathrm{h}}(t) = \frac{\mathrm{d}Q_{\mathrm{h}}}{\mathrm{d}t} = \frac{e_0}{d_{\mathrm{pn}}}\frac{x_0}{\tau_{\mathrm{h}}}e^{-t/\tau_{\mathrm{h}}}. \tag{3.10}$$

3.2 Overview of Common Semiconducting Detectors

We now briefly summarize some common semiconductor detectors...

3.2.1 Diffused-Junction Diode

- A diffused-junction diode is made by diffusing n-type dopants into a p-type semiconductor. Note that the production process of applying donor dopants requires high temperature, and is thus technically non-trivial.
- The surface of original p-type semiconductor where the n-type dopants are applied becomes strongly n-doped; we denote the region of strong n-type concentration with n^+. The n^+ layer is largely nonsensitive for the purposes particle detection; typical widths are $d \sim 0.1$ to $1\,\mu\mathrm{m}$. Meanwhile, the diode's depletion region is sensitive to particle detection; its width is of micrometer order without biasing and millimeter order in the presence of a reverse bias.
- Diffused-junction detectors are fairly radiation-hard.

3.2.2 Surface Barrier Detectors

- Surface barrier detectors consist of a junction between a semiconductor and a conductor (e.g. a metal). We analyze surface barrier detectors in terms of various characteristic energy levels, including:
  - the Fermi energy for electrons in the conductor,
  - a vacuum energy level E_F sufficient for freeing electrons from the semiconductor,
  - an energy difference Φ_m ("m" for metal) equal to the difference in energy from vacuum to Fermi energy; Φ_m is essentially the work function for removing an electron from the conductor.
  - the band gap E_g between the top of the valence band and bottom of the conducting band in the conductor and metal,
  - the semiconductor work function Φ_{sc} equal to the difference in vacuum energy and semiconductor Fermi energy.
  - Φ_b, the difference in vacuum energy in the metal and vacuum energy in the semiconductor; Φ_b plays the role of a potential energy barrier.

  When the conductor and semiconductor are placed together (in practice by diffusing semiconductor material onto a metal), the Fermi energy levels out and is constant across the semiconductor-metal boundary.
- At $T = 0\,\mathrm{K}$, the energy levels obey the following relationships:
  - The Fermi energy E_F is constant across the junction.
  - $E_F + \Phi_m$ reaches vacuum on the metal side.

    $E_F + \Phi_{sc}$ reaches vacuum on the semiconductor side.

  The various energies are related by

  $$E_F + \Phi_m - \Phi_b - \Phi_s = E_F \implies \Phi_b = \Phi_m - \Phi_{sc}.$$

  Takeaway: the semiconductor-conductor junction create a junction with a potential energy barrier between semiconductor and conductor sides. This junction then works like a pseudo p-n junction (which also has a potential energy barrier between p-type and n-type sides) and can be used for particle detection similarly to the depletion region of a p-n junction.
- For orientation: Some values of Φ_m and ϕ_b are given below

Metal	Φ_m [eV]	Metal-SC junction	Φ_b [eV]
Al	4.25	Al and n-type Ge	0.48
Au	4.80	Au and n-type Ge	0.59
-	-	Au and p-type Ge	0.30

  The height of this barrier Φ_b may be increased with reverse-biasing the metal-semiconductor junction.
- Surface-barrier detectors are also called Schottky diodes. For reference see https://en.wikipedia.org/wiki/Schottky_barrier and https://en.wikipedia.org/wiki/Metal-semiconductor_junction.

Remark: Creating Ohmic Contacts on Semiconductors

- A complication arises when making a contact (Ohmic contact) between a semiconductor and a conductor so that electrons (current) can freely flow from the semiconductor into the conductor? The problem arises because, as described above, joining a semiconductor and a metal (conductor) creates a Schottky diode with a potential energy barrier?
- Solution: apply a very thin layer of concentrated n^+ material onto a regular n-type semiconductor conductor, then apply a conductor onto the n^+ layer. Adding the n^+ layer makes the width (in position space) of the potential energy barrier between metal and semiconductor very narrow, which leads to large probability for tunneling of electrons from semiconductor into conductor, allowing current flow.

3.2.3 Compensated Semiconductor Detectors

Quoting from lecture, the construction of a compensated semiconductor detector beings with a basic p-n junction. The temperature is then greatly increased and an electric field applied in the direction from n-type to p-type. The temperature increase causes diffusion of positive donor ion cores further into the p-type side of depletion region. The net positive charge of these donor cores "cancels" the net negative charge of the acceptor cores in the depletion region. The net result is an electrically neutral region in center of junction with $\rho = 0$ without both free charge carriers or bound charges

In sequence from p-type to n-type, the above procedure produces: (i) neutral p-type semiconductor, (ii) a thin region with positive bound charge density (acceptor core, acceptor hole, donor core), (iii) electrically-neutral compensated region (like an intrinsic semiconductor), (iv) a thin region with negative bound charge density (donor core, donor electron, acceptor core) (v) electrically neutral n-type semiconductor.

The width of the neutral compensated layer is $d_\mathrm{i} \approx 10$ to $15\,\mathrm{mm}$, which is much larger than p-n junction width, which reaches at most millimeter order in the presence of external biasing. The large d_i creates a large region for potential particle detection, but also causes large leakage current, which requires cooling to low temperatures to reduce noise.

Reference: https://en.wikipedia.org/wiki/PIN_diode

3.2.4 Silicon-Lithium and Germanium-Lithium Detectors

- Silicon-Lithium (Si-Li) and Germanium-Lithium (Ge-Li) detectors are created by diffusing lithium from all sides into a p-type semiconductor. The result is a small p-type region surrounded by a large i-type region, with a small n^+ region on the surface layer.
- Define "soft" x-rays as energy $E_\gamma \in (1\,\mathrm{eV}, 10\,\mathrm{keV})$ and "hard" x-rays as energy $E_\gamma \in (10\,\mathrm{keV}, 100\,\mathrm{keV})$.

Si-Li Detectors

- Si-Li are used to detect soft x-rays. Reason: for photon energies $E_\gamma \lesssim 50\,\mathrm{keV}$, the photoelectric effect is the dominant photon-matter interaction process in silicon. Quoting from lecture, where the photoelectric effect dominates, photoelectrons leave their entire energy in the detector material. (Wouldn't it be: incident photon energy goes towards producing photoelectrons, which are detectable (as opposed to energy

going towards e.g. Compton scattering)?) In any case, all photon energy is deposited in the detector in a measurable form, which results in good energy resolution (recall energy resolution improves as E_{dep} approaches the incident particle's kinetic energy. Thus Si-Li semiconductor detectors are used for photon spectroscopy.

- Additionally, Si-Li detectors are used for electron spectroscopy (basically a fancy word for energy measurement) for electron energies in the range 0.1 to 5 MeV.

  Note that range of electrons in Si at 50 keV energy is of the order 20 µm. This is fairly small for a detector of the order e.g. millimeter width which is easily achievable. Lesson: in such a situation for a wide detector most electrons will fully stop, deposit all energy, and energy resolution for electron spectroscopy is good.

Ge-Li

- Ge-Li are used to detect higher-energy gamma rays, with energies at x-ray energies and above. Germanium is useful for high energy gamma rays because photon processes depend on the atomic number Z_{at} of the matter the photons interact with. Because germanium has a larger atomic number than silicon ($Z_{\text{Ge}} = 32$ and $Z_{\text{Si}} = 16$), Ge-Li are used for detecting higher-energy gamma rays.
- Quoting from lecture: the energy resolution in Ge-Li detectors for photons with incident energy of the order $E_{\text{dep}} \sim 1\,\text{MeV}$ falls in the range 10^{-4} to 10^{-5}.

Aside: Interpreting a Gamma Spectrum

Consider the gamma ray spectrum of the radioactive isotope ^{28}Al, which is known to decay via a 1.779 MeV gamma ray, as measured by a silicon gamma ray detector.

- The spectrum's photoelectric effect peak occurs at 1.779 MeV. Relevant physical process: a gamma ray from emitted by the ^{28}Al isotope is incident on a photon detector and creates and electron-hole pair with electron energy $E_{\text{e}} = 1.779\,\text{MeV}$ (technically minus electron-volt order work function, but this work function is of electronvolt order and is negligible). The photoelectron is fully absorbed in Si detector.
- The spectrum's Compton scattering plateau continues up to the Compton edge, which corresponds to the energy E_{max} for Compton scattering. For ^{28}Al the Compton edge occurs at about 1550 MeV.
- The spectrum will have a (very faint) single escape peak, which results from a gamma ray causing electron-positron pair production. The positron annihilates with an electron in the Si detector and produces two annihilation photons, each of energy 511 keV (the electron and positron rest energy). One of the annihilation photons registers in detector and one escapes undetected. In ^{28}Al the single escape peak occurs at $1.7789\,\text{MeV} - 511\,\text{keV}$.
- An analogous double escape peak occurs at $1.7789\,\text{MeV} - 2 \cdot 511\,\text{keV}$. In the ^{28}Al spectrum, the double escape peak is more prominent than single escape peak.
- Another small spectral peak occurs at 511 keV and results from electron-positron pair production caused by the initial gamma ray emitted by the ^{28}Al isotope. The electron may or may not be detected and is irrelevant to this peak, while the positron escapes the detector and annihilates in the surrounding housing. One of the two 511 keV annihilation photon happens to enter back into the Si detector and is fully absorbed.

4 Scintillation Detectors

- A *scintillator* is a material that outputs absorbed energy—in our case ionization energy deposited by an incident particle—in the form of visible light.

  Luminescence is the excitation of atomic energy levels and emission of visible light in the relaxation process. Luminescence is further divided into:

  (a) *fluorescence*, in which scintillation photons are emitted nearly immediately—of the order 1 to 10 ns—after energy absorption, and

  (b) *phosphorescence*, in which excited atomic states are metastable and scintillation photons are emitted after energy absorption. The time delay in phosphorescence between absorption and photon emission can vary considerably from microseconds to hours.

  Both fluorescence and phosphorescence involve the same phenomenon, but occur on different time scales. Note also that fluorescence and phosphorescence can occur simultaneously in the same material.

- The above times are understood to be measured from the time of energy absorption to the time of photon emission. In many scintillators, the time evolution of the number of scintillation photons N_γ after energy absorption is well-approximated by the exponentially-decaying model

$$\frac{\mathrm{d}N_\gamma}{\mathrm{d}t} = Ae^{-t/\tau_1} + Be^{-t/\tau_2}. \tag{4.1}$$

  The two terms encode "fast" and "slow" scintillation effects, and the time constants and relative amplitudes vary from material to material.

- Some advantages of scintillators in particle detectors include:
  - Rapid emission of photons in response to an incident particle
  - Linear response, meaning the number of scintillation photons is proportional to deposited particle energy.
  - Scintillators are (generally) simple to work with. (As opposed to, say, the complicated vacuum chambers and high voltages needed for gas-based detectors.)

- Some disadvantages of scintillators in particle detectors include:
  - Susceptibility to radiation damage
  - Non-organic scintillators are often hygroscopic (attract water from the surrounding environment) and must be used in waterproof housing
  - Only a small portion (of the order 10%) of deposited particle energy is converted to scintillation photons

4.1 Organic Scintillators

Mechanism for Luminescence in Organic Scintillators

- Scintillation arises from the energy transitions of delocalized electrons associated with an entire scintillator molecule (and not with a single atom). The ground state for

molecular electrons is a singlet state labeled S_0, above which are excited singlet states (e.g. S_1, S_2, etc...) and triplet states, labeled T_0, T_1, T_2, etc...

Additionally, imposed on each of the singlet and triplet states are finely-spaced energy levels associated with molecular vibrational modes.

Typical spacing between singlet energy levels is of the order 1 eV, while energy spacing between vibrational levels is of the order 0.1 eV.

- The scintillation process proceeds roughly as follows:

  1. A photon incident on the scintillator excites molecular electrons from the ground state S_0 the to the vibrational energy levels above S_1 (and not the vibrational levels above S_0!)

     If E_{in} denotes the energy of the incident photon, the balance of energy in the-above described process reads

     $$E_{\text{in}} = E_1 - E_0 + \Delta E_{\text{vib}}^{(1)} = E_{\text{e}}^*,$$

     where E_{e}^* is energy of excited electron, E_0 and E_1 are the energy levels of the singlet states S_0 and S_1, and $\Delta E_{\text{vib}}^{(1)}$ is the energy difference between the excited vibrational level and E_1.

  2. In a time of the order 1 ps, the excited molecular electron transitions without photon from the vibrational level above S_1 radiation to S_1 (the energy ΔE_{vib} is dissipated and heats the scintillator). At this point the molecular electron has energy

     $$E_{\text{e}}' = E_1 - E_0.$$

     The electron the relaxes into either (i) the S_0 ground state or (ii) a vibrational level above the S_0 ground state, and in the relaxation process emits a scintillation photon with energy

     $$E_{\text{scint}} = E_{\text{e}}' \qquad \text{or} \qquad E_{\text{scint}} = E_{\text{e}}' - \Delta E_{\text{vib}}^{(0)}, \tag{4.2}$$

     where $\Delta E_{\text{vib}}^{(0)}$ is the energy difference between the vibrational level and E_0.

  The difference in incident and scintillation photon energies is then

  $$E_{\text{in}} - E_{\text{scint}} = \left(E_1 - E_0 + \Delta E_{\text{vib}}^{(1)}\right) - (E_1 - E_0) = \Delta E_{\text{vib}}^{(1)} \qquad \text{or}$$
  $$E_{\text{in}} - E_{\text{scint}} = \left(E_1 - E_0 + \Delta E_{\text{vib}}^{(1)}\right) - \left(E_1 - E_0 - E_{\text{vib}}^{(0)}\right) = \Delta E_{\text{vib}}^{(1)} + E_{\text{vib}}^{(0)},$$

  depending on the process that occurs in Equation 4.2.

  Lesson: $E_{\text{scint}} < E_{\text{in}}$, which means the scintillation photon cannot re-excite more molecular electrons and thus leaves the scintillator material as visible light. (While $E_{\text{scint}} < E_{\text{in}}$ would lead to a recursive re-excitation process in which scintillation photons would never leave the material, and could not be used for particle detection).

  The above-described interactions between singlet states result in the fast component of phosphorescence in Equation 4.1.

Triplet States

- When an incident photon excites a molecular electron into a triplet state, the electron immediately decays into the ground triplet state T_0 in a non-radiative process. (Note that T_0 is still above is ground singlet state S_0).
- The transition directly from T_0 to S_0 is very unlikely because of selection rules. Instead, the T_0 state decays by first interacting with a second T_0 state in another molecule in the surrounding matter. This T_0-T_0 interaction reads

$$T_0 + T_0 \rightarrow S_1 + S_0 + h\nu_{\text{scint}}.$$

  In other words, the two T_0 states decay to the singlet ground state S_0 and the excited singlet state S_1 and emit a scintillation photon in the process.
- The $T_0 + T_0 \rightarrow S_1 + S_0$ interaction result in the slow component of luminescence in Equation 4.1.

Examples of Organic Scintillators

We now briefly summarize a few common types of organic scintillators.

- Anthracene is an organic material with the chemical formula $C_{14}H_{10}$. Anthracene requires about 60 eV for creation of a photon and has a time constant of the order $\tau \sim 30$ ns. The material converts about five percent of its energy to light.
- Organic fluids consist of an organic scintillating material dissolved in a fluid solvent. Organic fluids can be used as wavelength shifters, which are useful for moving scintillation photon wavelengths to an interval where photodetectors are more sensitive.
- Plastic scintillators consist of an organic scintillator dissolved in a solid solvent, and have a time constant of the order 1 ns. Since this very short time constant is comparable to the excitation time of the scintillating material itself as the incident particle travels through it, one must take into account excitation time when analyzing the scintillation dynamics.

  Plastic scintillators are convenient because their production and handling is relatively simple (although one must take care to avoid contact between plastic scintillators and organic solvents like acetone, and use gloves when handling to avoid contact with oils on the skin surface).

4.2 Inorganic Scintillators

Scintillation Mechanism

- In inorganic scintillators, scintillation occurs because of electron band structure in crystals (and not as a result of discrete molecular energy levels in organic scintillators). Because inorganic scintillators are insulators, the band gap between valence and conduction bands is of the order $E_g \sim 10$ eV (as opposed to $E_g \sim 1$ eV in semiconductors).

  Note that, like in semiconductors, inorganic scintillators contain a small concentration of impurities in addition to the scintillation material itself.
- A particle incident on an inorganic scintillator excites a scintillator electron from the valence band to the conduction band, resulting in an electron-hole pair.

  The hole then effectively ionizes an impurity atom, causing an electron from the impurity atom to move into the conduction band.

Electrons from the conduction band then relax into the vacated impurity state left behind by impurity electron. This relaxing conduction band electron radiates a photon with energy less than the incident particle. This radiated photon lacks the energy to create a new electron-hole pair and leaves the scintillator material as a detectable scintillation photon.

Properties

- Inorganic scintillators generally have slow response time, of the order 100 ns (although lead tungstate has a response time of the order 10 ns).
- Inorganic scintillators are often hydrophilic and require external housing to prevent contact with water in the environment's air.
- Inorganic scintillators are usually made of materials with large atomic number, resulting in large ionizing energy losses and thus better energy resolution than typical organic scintillators.

4.3 On Linearity of Scintillating Detectors

- For the most part, scintillators have a linear response. In symbols, we might write this as

$$\frac{\mathrm{d}N}{\mathrm{d}x} \propto \frac{\mathrm{d}E}{\mathrm{d}x}, \tag{4.3}$$

  where the number of scintillation photons emitted per unit distance traveled by an incident particle through the scintillator is proportional to the particle's ionizing energy losses $\frac{\mathrm{d}E}{\mathrm{d}x}$.
- This linearity breaks down for low energy particles, for which so-called "quenching interactions" result in loss of linearity. For orientation, quoting from lecture, most scintillators have a linear response for electron energies above $T_\mathrm{e} \gtrsim 125\,\mathrm{keV}$ and proton energies above $T_\mathrm{p} \gtrsim 5\,\mathrm{MeV}$.
- Quenching interactions are more likely for a high density of excited molecules.

  Recall that ionizing energy losses increase as a particle slows (i.e. as a particle's kinetic energy decreases). Resultantly, lower-energy particles have higher ionizing losses and thus generate a higher density of excited molecules, causing quenching interactions and loss of linearity.

  In this regime the linear relationship in Equation 4.3 can be approximated as

$$\frac{\mathrm{d}N}{\mathrm{d}x} = \frac{a\frac{\mathrm{d}E}{\mathrm{d}x}}{1 + b\frac{\mathrm{d}E}{\mathrm{d}x}},$$

  where a and b are phenomenologically-determined constants.

5 Classifying Particles By Mass

All charged elementary particles typically observed in particle detectors have relatively well-separated masses, i.e. no common particles have masses very close to each other. For example:

Particle	Mass $[\mathrm{MeV/c^2}]$
Electrons	≈ 0.5
Pions	≈ 140
Kaons	≈ 490
Protons	≈ 940

Because familiar particles have different masses, we can classify the identity of unknown particles by measuring the particle's mass. In other words, in many cases, particle identification essentially reduces to mass measurement.

Measuring Mass

- It is possible to determine a particle's mass from independent measurements of its momentum p and speed β.
- As a simple example, one can measure a particle's momentum from the curvature of its trajectory in a transverse magnetic field, as mentioned in the introduction of Section 2.6 on position-sensitive detectors. In the simplest two-dimensional case, a particle's transverse momentum relative to a magnetic field is found from the trajectory's radius of curvature R via

  $$m\frac{v^2}{R} = qvB \implies p_\mathrm{T} = qBR;$$

  note, however, that this method only computes the particle's transverse momentum, i.e. the momentum component perpendicular to the magnetic field.
- To find the particle's mass, we then recall the relativistic relations

  $$E = \gamma mc^2 \qquad \text{and} \qquad \gamma = \frac{1}{\sqrt{1-\beta^2}},$$

  which we rearrange to get

  $$E = \frac{mc^2}{\sqrt{1-\beta^2}} \implies \beta^2 = 1 - \frac{m^2c^4}{E^2}.$$

  We then use the special relativity energy relationship

  $$E = p^2c^2 + m^2c^4$$

  together with $\beta = \frac{v}{c} = \frac{cp}{E}$ to get

  $$\beta = \frac{cp}{E} = \frac{cp}{\sqrt{c^2p^2 + m^2c^4}} \implies m^2c^4 = \frac{p^2c^2}{\beta^2}(1-\beta^2).$$

  Assuming momentum pc and speed β are known independently, we can find the particle's mass with the above equation.

Another Approach Using Energy and Momentum

- It is also possible to determine particle mass from independent measurements of momentum p and kinetic energy T (which can be measured in a calorimeter).

  In this case, the relevant equation is

$$m^2c^4 = E^2 - p^2c^2 = (T + mc^2)^2 - p^2c^2 \implies mc^2 = \frac{p^2c^2 - T^2}{2T}.$$

5.1 Multiple Measurements of Ionizing Losses

- It is also possible to estimate particle mass from repeated measurements of the particle's ionizing energy losses in matter. For review from Equation 1.7, a heavy charged particle's ionizing losses in matter are well-approximated by the Bethe formula

$$-\frac{\mathrm{d}E}{\mathrm{d}x} = \frac{4\pi}{m_\mathrm{e}c^2} \cdot \frac{n_\mathrm{e}z^2}{\beta^2} \cdot \left(\frac{e_0^2}{4\pi\epsilon_0}\right)^2 \left[\ln\left(\frac{2m_\mathrm{e}c^2\gamma^2\beta^2}{I}\right) - \beta^2\right].$$

  For our purposes, it is enough to note that in the low-energy regime, ionizing losses obey the proportionality

$$\left\langle \frac{\mathrm{d}E}{\mathrm{d}x} \right\rangle \sim \frac{1}{\beta^2} \qquad \text{(for low } \beta\text{)}.$$

- A heavier particle at a given momentum cp will have smaller speed β than a lighter particle. At smaller speed, ionizing losses are larger (in the $\left\langle \frac{\mathrm{d}E}{\mathrm{d}x} \right\rangle \sim 1/\beta^2$ regime).

  Determining mass via ionizing losses then works on the following simple principle:

  - The momentum cp of the to-be-classified particle must be known; knowing momentum is usually possible if one knows the parameters of the accelerator used to accelerate the particle.
  - Measure the ionizing losses of to-be-classified particle.
  - At a given momentum cp, particles with larger mass have larger values of ionizing losses, and thus ionizing losses can be used to classify two species of particles.

- Importantly, ionizing losses are a random variable. In other words, the same particle with the same mass and momentum passing through the same detector will have different ionizing losses during each experiment, centered around a mean value $\frac{\mathrm{d}E}{\mathrm{d}x}$.

  Conclusion: we must take multiple measurements of ionizing losses during any given experiment, and then average these measurements to estimate the expected value $\frac{\mathrm{d}E}{\mathrm{d}x}$. In practice, experiments could also use a series of independent ionizing detectors placed one after the other.

  Alternatively, averaging the signals from each wire of a multi-wire proportional chamber can also give an estimate of $\frac{\mathrm{d}E}{\mathrm{d}x}$.

- Note that multiple measurements of ionizing losses are effective only at relatively low particle momenta, for the following reasons:

  1. The $\frac{\mathrm{d}E}{\mathrm{d}x} \sim 1/\beta^2$ regime holds only for $\beta \lesssim 0.95$.
  2. Resolution of momentum measurements decreases with increasing particle momentum.

Statistical Distribution of Ionizing Losses

- Ionizing losses $\frac{\mathrm{d}E}{\mathrm{d}x}$ for particles at a given mass and kinetic energy are distributed according to a Landau distribution—this distribution has a roughly Gaussian peak, but unlike the normal distribution, the Landau distribution is a so-called "fat-tailed" distribution.

  Although the exact probability density function for the Landau distribution is complicated and impractical for numerical computations, a good approximation is

$$L(x) \approx \frac{1}{\sqrt{2\pi}} \exp\left[-\frac{1}{2}(x + e^{-x})\right].$$

- Suppose we take N measurements of a Landau-distributed variable x, where each measurement carries an uncertainty σ_x. In this case, without proof, the uncertainty of the average value $\overline{x}$ improves to

$$\sigma_{\overline{x}} \propto \frac{1}{N^{\alpha}}, \quad \text{where } \alpha < 1/2.$$

  For review, the analogous expression for a Gaussian distributed variable would be

$$\sigma_{\overline{x}} = \frac{1}{\sqrt{N}} = \frac{1}{N^{1/2}}. \qquad \text{(for a Gaussian variable)}$$

  In other words (as a result of the Landau distribution's fat tail), the uncertainty of a Landau-distributed variable decreases (i.e. improves) more slowly with increasing measurements N than a Gaussian-distributed variable.

- We often work with a truncated mean: loosely, this is a compromise in which we consider only the momentum measurements in the central, approximately Gaussian regime of the Landau distribution and reject measurements from the "fat-tailed" regimes. For example, one might considers only the smallest 50% (roughly) of the measurements. We take the smaller measurements because these fall into the Landau distribution's roughly Gaussian regime, and (approximately) obey the Gaussian combination rule

$$\sigma_{\overline{x}} \approx \frac{1}{\sqrt{N}}.$$

  Using a truncated mean is a compromise—we have fewer measurements available to perform statistics, but it causes uncertainty of the mean to fall faster with increasing number of measurements.

5.2 Time-of-Flight Measurement

- Time-of-flight detectors first measure the time Δt for for different particles to travel a known distance. This difference in times can be used to determine the difference in particle masses, as derived below.

- The difference in time of flight for two different particles, one traveling at speed v_1 and one at speed v_2, through the same detector of length L is simply

$$\Delta t = \frac{L}{v_1} - \frac{L}{v_2} = \frac{L}{\beta_1 c} - \frac{L}{\beta_2 c}. \tag{5.1}$$

We then find an expression for $1/\beta$ using the relativistic relations

$$\frac{1}{\beta} = \frac{E}{cp} = \frac{\sqrt{c^2p^2 + (mc^2)^2}}{cp} = \sqrt{1 + \frac{(mc^2)^2}{c^2p^2}}.$$

We then substitute this expression into Equation 5.1 to get the time difference

$$\Delta t = \frac{L}{c}\left(\sqrt{1 + \frac{(m_1c^2)^2}{c^2p^2}} - \sqrt{1 + \frac{(m_2c^2)^2}{c^2p^2}}\right).$$

Note the assumption that both particles are known to have the same momentum cp. We then consider the relativistic limit $cp \gg mc^2$ and Taylor-expand the square roots to first order in $(mc)/p$ to get

$$\begin{aligned}\Delta t &= \frac{L}{c}\left(\sqrt{1 + \frac{m_1^2c^2}{p^2}} - \sqrt{1 + \frac{m_2^2c^2}{p^2}}\right) \\ &\approx \frac{L}{c}\left[1 + \frac{m_1^2c^2}{2p^2} - \left(1 + \frac{m_2^2c^2}{2p^2}\right)\right] \\ &= \frac{Lc}{p^2}(m_1^2 - m_2^2) = \frac{Lc}{p^2}(m_1 - m_2)(m_1 + m_2).\end{aligned}$$

We then introduce the mass difference $\Delta m \equiv m_1 - m_2$ and average mass $\overline{m} \equiv (m_1 + m_2)/2$, in terms of which the time difference reads

$$\Delta t = \frac{Lc}{p^2}\Delta m \cdot 2\overline{m} \implies \Delta m = \Delta t \frac{p^2}{Lc}\frac{1}{2\overline{m}}.$$

Lesson: we can determine the difference in mass between two particles (at a given momentum p and assuming the average mass is known beforehand) from the time-of flight measurement Δt.

- The uncertainty $\sigma_{\Delta m}$ in the mass measurement in terms of the uncertainty $\sigma_{\Delta t}$ in the time difference measurement is

$$\sigma_{\Delta m} = \frac{p^2}{Lc}\frac{1}{2\overline{m}}\sigma_{\Delta t}. \tag{5.2}$$

This expression allows us to estimate the required time resolution for a desired mass resolution. Note that the mass resolution in Equation 5.2 increases with p^2. Thus, for example, doubling particle momentum requires the detector length L increase by a factor of four to maintain a given mass resolution. As a result, time-of-flight detectors quickly grow impractical at large particle momenta.

Example: Pions and Kaon

Consider an experiment in which both pions (mass $m_\pi c^2 \approx 140\,\text{MeV}$) and kaons (mass $m_K c^2 \approx 490\,\text{MeV}$) have momentum $cp = 1\,\text{GeV}$. The scintillators used to make the time-of-flight measurement are separated by a distance $L = 0.5\,\text{m}$, and the associated time resolution is known to be $\sigma_{\Delta t} \sim 0.3\,\text{ns}$.

In this case

$$\frac{\sigma_{\Delta m}}{\overline{m}} = \frac{p^2}{Lc}\frac{1}{2\overline{m}^2}\sigma_{\Delta t} \approx 0.302 \sim 1/3.$$

We interpret this result as a 3σ classification significance between pions and kaons.

5.3 Cherenkov Radiation

5.3.1 The Cherenkov Angle

- A charged particle moving through a dielectric material with refractive index n at speed $v > c_0/n$ (i.e. a speed greater than the phase velocity of light in the material) will emit Cherenkov radiation, where c_0 is the speed of light in vacuum.
- Mechanism: in general, for any particle speed v, a charged particle passing through material polarizes and excites the surrounding molecules. The polarized molecules emit photons in relaxation process. For $v > c_0/n$, the distribution of polarization in the surrounding matter is asymmetric along the direction of particle motion. Photons emitted from this asymmetric distribution in the relaxation process interfere to form the conical Cherenkov wavefront.
- Geometry and coordinate system (best to see a picture): Consider a particle moving along the positive x axis at speed $v > c_0/n$, The particle's Cherenkov radiation wavefronts appear as cones centered around the x axis, with the vertex at the instantaneous particle position and spreading backwards along the x axis. The angle between the normal to cone surface and the x axis is called the *Cherenkov angle* and is denoted by θ_C.

  In time t, light travels a distance $s_\mathrm{light} = (c_0/n)t$ from a point a distance $x = vt$ behind the instantaneous particle position on the x axis to a point on the cone surface (along a path normal to the cone line). This consideration leads to the relationship

$$\cos\theta_\mathrm{C} = \frac{s_\mathrm{light}}{x} = \frac{(c_0/n)t}{vt} = \frac{1}{n\beta}, \quad \text{where } \beta \equiv \frac{v}{c_0}.$$

  The Cherenkov angle is thus given by

$$\cos\theta_\mathrm{C} = \frac{1}{n\beta} \implies \theta_\mathrm{C} = \cos^{-1}\frac{1}{n\beta}. \tag{5.3}$$

- The Cherenkov angle (because of the inverse cosine function) is defined only for $1/(n\beta) < 1$, which gives a threshold speed

$$\frac{1}{n\beta} < 1 \implies \beta > \frac{1}{n} \qquad \text{(threshold for Cherenkov radiation).}$$

  In terms of momentum, using $\gamma\beta = (pc)/(mc^2)$, the Cherenkov threshold reads

$$\beta = \frac{pc}{\gamma mc^2} = \frac{pc}{E} = \frac{pc}{\sqrt{m^2c^4 + p^2c^2}} > \frac{1}{n} \implies pc > \frac{mc^2}{\sqrt{1 - 1/n^2}}. \tag{5.4}$$

5.3.2 Cherenkov Photon Frequency and Wavelength Spectra

Frequency Spectrum

- Without derivation, we quote that the Maxwell equations lead to a radiated Cherenkov photon energy spectrum (per unit length traveled by a radiating particle through detector material) given by

$$\frac{\mathrm{d}^2E}{\mathrm{d}x\,\mathrm{d}\omega} = z^2\frac{\alpha\hbar\omega}{c}\sin^2\theta_\mathrm{C}, \tag{5.5}$$

  where $\alpha = 1/137$ is the fine structure constant, z is the incident particle's charge in units of e_0, and ω is frequency of radiated energy.

- Using the photon energy formula $E_\gamma = \hbar\omega$, the energy of N Cherenkov photons at the frequency ω is

$$E = N\hbar\omega \implies N = \frac{E}{\hbar\langle\omega\rangle} \implies \frac{\mathrm{d}N}{\mathrm{d}E} = \frac{1}{\hbar\langle\omega\rangle}.$$

  Using $\frac{\mathrm{d}N}{\mathrm{d}E}$, we then convert Equation 5.5 to a distribution over N via

$$\frac{\mathrm{d}^2N}{\mathrm{d}x\,\mathrm{d}\omega} = \frac{\mathrm{d}^2E}{\mathrm{d}x\,\mathrm{d}\omega}\frac{\mathrm{d}N}{\mathrm{d}E} = \left(z^2\frac{\alpha\hbar\omega}{c}\sin^2\theta_\mathrm{C}\right)\cdot\frac{1}{\hbar\omega} = \frac{z^2\alpha}{c}\sin^2\theta_\mathrm{C}.$$

  Finally, we express $\sin^2\theta_\mathrm{C}$ from Equation 5.3 and the use the identity $\sin^2 x = 1-\cos^2 x$ to write the Cherenkov photon frequency spectrum as

$$\frac{\mathrm{d}^2N}{\mathrm{d}x\,\mathrm{d}\omega} = \frac{z^2\alpha}{c}\sin^2\theta_\mathrm{C} = \frac{z^2\alpha}{c}\left(1-\frac{1}{(n\beta)^2}\right). \tag{5.6}$$

Wavelength Spectrum

- Finally, we aim to derive $\frac{\mathrm{d}^2N}{\mathrm{d}x\,\mathrm{d}\lambda}$, the distribution of the number of radiated Cherenkov photons (per unit distance traveled) with respect to wavelength.
- We begin with the wavelength-frequency relationship

$$\omega = 2\pi\frac{c}{\lambda} \implies \frac{\mathrm{d}\omega}{\mathrm{d}\lambda} = \frac{2\pi c}{\lambda^2},$$

  which we then substitute into Equation 5.6 to get

$$\frac{\mathrm{d}^2N}{\mathrm{d}x\,\mathrm{d}\lambda} = \frac{\mathrm{d}^2N}{\mathrm{d}x\,\mathrm{d}\omega}\frac{\mathrm{d}\omega}{\mathrm{d}\lambda} = \frac{2\pi z^2\alpha}{\lambda^2}\left(1-\frac{1}{(n\beta)^2}\right) = \frac{2\pi z^2\alpha}{\lambda^2}\sin^2\theta_\mathrm{C}. \tag{5.7}$$

- Note that, more generally, the refractive index n is a function of wavelength (or frequency), so both this formula and Equation 5.6, which treat n as a constant, are not perfectly accurate.

Estimating the Number of Detected Cherenkov Photons

- Consider a Cherenkov radiation detector of length L using a radiating material of refractive index n. Note that in practice, detectors are sensitive to photons only in a certain frequency (or wavelength) range, typically for photon wavelengths in the range 300 to 700 nm; we model the detector's limited bandwidth with an efficiency function $\eta(\lambda)$.
- In general the number of photons registered by a Cherenkov detector is estimated by integrating the radiated Cherenkov photon spectrum times the detector efficiency over the detector's responsive wavelength range, i.e.

$$N_\mathrm{det} = L\int_{\lambda_\mathrm{min}}^{\lambda_\mathrm{max}}\eta(\lambda)\frac{\mathrm{d}^2N}{\mathrm{d}x\,\mathrm{d}\lambda}\,\mathrm{d}\lambda = 2\pi z^2\alpha L\int_{\lambda_\mathrm{min}}^{\lambda_\mathrm{max}}\eta(\lambda)\frac{\sin^2\theta_\mathrm{C}}{\lambda^2}\,\mathrm{d}\lambda.$$

5.3.3 Threshold Cherenkov Detectors

- Threshold Cherenkov detectors are based on the principle that at a given momentum pc in a material with a properly chosen refractive index n, one species of particle will emit Cherenkov radiation while a different species, with larger mass, will not.

  Particles can then be classified from the emission of Cherenkov (or the lack of it).

- More concretely, consider two species of ionizing particles with masses $m_2 > m_1$, so that at a given momentum $\beta_2 < \beta_1$. To classify these particles, we choose a refractive index n such that $n\beta_1 \geq 1$ and $n\beta_2 \leq 1$, i.e.

$$\frac{1}{\beta_1} \leq n \leq \frac{1}{\beta_2}.$$

  Typically a detector would use the threshold value $n = 1/\beta_2$ (the maximum possible value of n such that particles of mass m_2 still do not radiate), since a larger n leads to a larger number of detected photons via

$$\frac{N_\gamma}{L} \propto \sin^2\theta_\mathrm{C} = 1 - \frac{1}{n^2\beta^2}.$$

  For a material with $n = 1/\beta_2$, and setting $\beta = \beta_1$ the number of detected photons obeys

$$\frac{N_\gamma}{L} \propto \sin^2\theta_\mathrm{C} = 1 - \frac{1}{n^2\beta^2} = 1 - \frac{\beta_2^2}{\beta_1^2}. \tag{5.8}$$

  We then recall the relativistic relationship

$$\beta = \frac{v}{c} = \frac{cp}{E} = \frac{cp}{\sqrt{(mc^2)^2 + (cp)^2}},$$

  which we Taylor expand in relativistic regime $cp \gg mc^2$ to get

$$\beta \propto 1 - \frac{(mc^2)^2}{2(cp)^2}.$$

  We then substitute this expression for β into Equation 5.8 to get

$$\begin{aligned}\frac{N_\gamma}{L} \propto 1 - \frac{\beta_2^2}{\beta_1^2} &\approx 1 - \left(1 - \frac{m_2^2c^4}{2c^2p^2}\right)\cdot\left(1 + \frac{m_1^2c^4}{2c^2p^2}\right) \\ &\approx 1 - \left(1 + \frac{m_1^2 - m_2^2}{2p^2}c^2\right),\end{aligned}$$

  where we have neglected the higher-order term $(m_1^2m_2^2c^8)/(4c^4p^4)$. The result, after rearranging slightly, is

$$N_\gamma \propto \frac{m_2^2 - m_1^2}{2c^2p^2}c^4L.$$

  Lesson: The number of emitted Cherenkov photons falls quadratically with particle momentum cp, which means the radiative material length L required to maintain a given N_γ quickly grows impractically large with increasing particle momentum. The result is similar to the dilemma discussed for time-of-flight detectors in the context of Equation 5.2.

5.3.4 Ring-Imaging Cherenkov Detector

Ring-Imaging Cherenkov (RICH) detectors are used to determine particle speed β by measuring the Cherenkov angle θ_C of the particle's Cherenkov radiation. If θ_C and the refractive index n of the detector's radiative material are known, β is easily found, in principle, from

$$\cos\theta_C = \frac{1}{n\beta} \implies \beta = \frac{1}{n\cos\theta_C}.$$

Resolution With Ring Cherenkov Detectors

- We now aim to estimate the how the resolution in a measurement of Cherenkov angle θ_C affects the resolution of a corresponding measurement of particle mass m. We begin with the defining Cherenkov angle relationship

  $$\cos\theta_C = \frac{1}{\beta n},$$

  and take the total differential of both sides to get

  $$\mathrm{d}\big[\cos\theta_C\big] = -\frac{\mathrm{d}\beta}{\beta^2 n}. \tag{5.9}$$

  Recall that, for $cp \gg mc^2$, particle speed β is given by

  $$\beta = 1 - \frac{(mc^2)^2}{(cp)^2} \implies \mathrm{d}\beta = -\frac{c^2 m\,\mathrm{d}m}{p^2}.$$

  We then substitute this expression for $\mathrm{d}\beta$ into Equation 5.9 to get

  $$\mathrm{d}\big[\cos\theta_C\big] = \frac{c^2 m}{p^2\beta^2 n}\,\mathrm{d}m = \frac{c^4 m}{p^2 c^2}\frac{\mathrm{d}m}{\beta^2 n}.$$

  We then make two approximations: $\beta \lesssim 1$ for fast particles and $n \gtrsim 1$ for typical detector materials. These approximations produce

  $$\mathrm{d}\big[\cos\theta_C\big] \approx \frac{c^4 m}{c^2 p^2}\,\mathrm{d}m.$$

  Uncertainty in mass σ_m is thus related to uncertainty in Cherenkov angle $\sigma_{\cos\theta_C}$ via

  $$\theta_{\cos\theta_C} = \frac{c^4 m}{c^2 p^2}\sigma_m \implies \sigma_m = \frac{c^2 p^2}{mc^4}\sigma_{\cos\theta_C}.$$

  In particular, we note that mass resolution worsens (grows larger) with increasing particle momentum.

5.4 In Passing: Transition Radiation

- We now *very briefly* outline a phenomenon called transition radiation.

  Transition radiation occurs when a charged particle emits photons upon passing through an interface between two materials with different refractive indices n_1 and n_2.

- The angle of refraction for transition radiation is not well-defined (unlike the Cherenkov angle), but distributed around a central value. We simply quote that the refraction angle distribution's central value θ obeys

$$\theta \sim \frac{1}{\gamma}$$

- Importantly, the total number of emitted transition radiation photons for a particle traveling with Lorentz factor γ scales linearly as

$$N \propto \gamma,$$

  so the number of photons can be used as an estimate of particle speed.

- Consideration: radiated photons are absorbed in material; we can increase the number of transition radiation photons by using many consecutive layers of alternating transition radiation material.

5.5 Summary of Classification Methods

Momenta $pc \leq 1\,\mathrm{GeV}$

- Possible method: multiple measurements of ionizing losses

  Limitations: $\left\langle \frac{\mathrm{d}E}{\mathrm{d}x} \right\rangle$ reaches a minimum at large momenta (at $\gamma \approx 4$ for all particles; about $pc \sim 500\,\mathrm{MeV}$ for pions). In the MIP regime there are no significant differences in ionizing losses for different particles.

- Possible method: time-of-flight detectors

  Limitation: the $L \propto p^2$ relationship at a given resolution makes time-of-flight detectors impractical for momenta larger than about $pc \approx 1\,\mathrm{GeV}$.

Momenta in the Range $pc \in 1.5$ **to** $10\,\mathrm{GeV}$

- Possible method: multiple measurements of ionizing losses with relativistic corrections
- Limitation: at large momenta, $\left\langle \frac{\mathrm{d}E}{\mathrm{d}x} \right\rangle$ must be measured with high resolution to separate masses

  Quoted example: At $pc \approx 100\,\mathrm{GeV}$, classifying kaons and pions requires $\left\langle \frac{\mathrm{d}E}{\mathrm{d}x} \right\rangle$ be measured with 2% relative uncertainty.

Momenta $pc \leq 25\,\mathrm{GeV}$

- Possible method: threshold Cherenkov radiation detectors
- Limitation: the number of emitted photons scales as $N \sim \frac{L}{p^2}$. Maintaining detectable amounts of photons at large momenta requires impractically long detectors.

Momenta $pc \leq 50\,\mathrm{GeV}$

- Possible method: ring-imaging Cherenkov detectors
- Limitations: achieving good resolution $\sigma_{\theta_\mathrm{C}}$ in the Cherenkov angle measurement is difficult in practical experiments, and varies finely with detector geometry and aberrations in the measurement instruments.

Momenta $pc \geq 100\,\mathrm{GeV}$

- Possible method: transition radiation detectors
- Limitation (at low momenta): the number of emitted transition radiation photons scales as $N \sim \gamma$.

6 Neutron Detection

In this section we briefly outline the basics of neutron detection. We detect neutrons indirectly, from their decay products. General plan: (i) first be aware of common neutron interactions and learn these interactions' decay products, then (ii) search for these decay products, which are more easily detected than neutrons themselves.

6.1 Slow Neutrons

- For slow (also called thermal) neutrons, which have kinetic energies in the range $T_\mathrm{n} \lesssim 0.1\,\mathrm{eV}$, two common reactions are

$$^3\mathrm{He} + n \to {}^3\mathrm{H} + {}^1\mathrm{H} \qquad \text{and} \qquad {}^{10}\mathrm{B} + n \to {}^7\mathrm{Li} + {}^4\mathrm{He}.$$

- As an example, a possible neutron detector could involve a gas detector with a mixture of ^{3}He and BF_3. The detector must be shielded from non-neutron ionizing radiation to avoid false positive neutron measurements. Such a shield is often made of lead—for orientation, quoting from lecture, a 5 cm layer of lead absorbs roughly 0.1% of incident 1 MeV neutrons and 90% of 1 MeV photons.

- For orientation: in a cylindrical detector of radius $R = 5\,\mathrm{cm}$ filled with BF_3 at a pressure of $0.7 \cdot 10^5\,\mathrm{Pa}$, the probability for interaction with a thermal neutron is about 30%, while probability for interaction with a 1 MeV photon is only about 0.06%.

  For comparison, in an argon-filled cylindrical detector with radius $R = 2.5\,\mathrm{cm}$ at a pressure of $2 \cdot 10^5\,\mathrm{Pa}$, the probability for interaction with thermal neutrons is essentially zero, and the probability for interaction with a 1 MeV photon is roughly 0.05%. Lesson: BF_3 is good for neutron detection and won't detect gamma rays!

6.2 Fast Neutrons

Fast neutrons have low interaction probability and are thus difficult to detect. Solution: slow down fast neutrons to thermal energies by collisions with absorbing matter, then detect the slow neutrons with the processes outlined above.

6.2.1 Post-Scattering Energy Distribution of Fast Neutrons

- We will first determine the energy distribution of a fast neutron with initial energy $E \gg k_B T$ after a single scattering from the nucleus of an element with mass number A. Working in a classical, non-relativistic regime, consider a neutron with velocity v_1 and mass m incident on a stationary nucleus with mass $M \approx A \cdot m$. The velocity of the neutron-nucleus system's center of mass is

$$v^* = \frac{mv_1}{m+M} = \frac{mv_1}{m+Am} = \frac{v_1}{A+1}, \tag{6.1}$$

  while the neutron and nucleus's velocities in the center of mass frame are

$$v_1^* = v_1 - v^* = \frac{A}{A+1}v_1 \qquad \text{and} \qquad v_2^* = 0 - v^* = -\frac{v_1}{A+1}. \tag{6.2}$$

- In the center of mass (CoM) frame, conservation of energy and momentum produce the post-collision relationships

$$\left|\mathbf{v}_1'^*\right| = |\mathbf{v}_1^*| \qquad \text{and} \qquad \left|\mathbf{v}_2'^*\right| = |\mathbf{v}_2^*|.$$

In other words, the magnitudes of each particles' CoM-frame velocity are preserved; only the velocity directions change.

- Transforming to the lab frame, the neutron's velocity after collision is

$$\mathbf{v}_1' = \mathbf{v}^* + \mathbf{v}_1'^*.$$

Using $\mathbf{v}_1'$, we aim to find the neutron's energy after the collision. Since $E \propto v_1'^2$, we first compute

$$v_1'^2 = (\mathbf{v}^* + \mathbf{v}_1'^*)(\mathbf{v}^* + \mathbf{v}_1'^*) = (v^*)^2 + 2v^* v_1^* \cos\theta' + (v_1^*)^2,$$

where θ is the angle between initial and final neutron direction in the center-of mass frame. We then substitute in v^* and v_1^* from Equations 6.1 and 6.2 to get

$$v_1'^2 = \frac{v_1^2}{(A+1)^2} + 2\frac{v_1}{A+1}\frac{Av_1}{A+1}\cos\theta + \frac{A^2 v_1^2}{(A+1)^2} = \frac{A^2 + 2A\cos\theta + 1}{(A+1)^2} v_1^2.$$

The ratio of the neutron's pre- and post-collision energy is then

$$\frac{E'}{E} = \frac{v_1'^2}{v_1^2} = \frac{A^2 + 2A\cos\theta + 1}{(A+1)^2}.$$

Since $\cos\theta \in [-1, 1]$, the maximum and minimum post-scattering energies are

$$E'_{\max} = E \qquad \text{and} \qquad E'_{\min} = \frac{(A-1)^2}{(A+1)^2} E \equiv \alpha E, \tag{6.3}$$

where we have defined the coefficient

$$\alpha \equiv \frac{(A-1)^2}{(A+1)^2}. \tag{6.4}$$

Note that maximum post-collision energy, which occurs when $\cos\theta = 1 \implies \theta = 0$, corresponds to no scattering at all, while minimum energy, when $\theta = \pi$, corresponds to perfect neutron back-scattering.

- Additionally, note that stopping is most efficient if mass of the absorbing particle equals the neutron mass, i.e. if $M = m$ or $A = 1$, in which case $E'_{\min} \to 0$.

The condition $A = 1$ is met in hydrogen, so absorber materials typically contain a large proportion of hydrogen.

Post-Scattering Energy Distribution

- For review, the neutron's post-collision energy depends on scattering angle as

$$\frac{E'}{E} = \frac{v_1'^2}{v_1^2} = \frac{A^2 + 2A\cos\theta + 1}{(A+1)^2}.$$

Plan: find the neutron's post-collision energy distribution from the distribution of the scattering angle θ using the chain rule

$$\frac{\mathrm{d}P}{\mathrm{d}E'} = \frac{\mathrm{d}P}{\mathrm{d}[\cos\theta]} \cdot \frac{\mathrm{d}[\cos\theta]}{\mathrm{d}E'}.$$

We first compute

$$\frac{\mathrm{d}[\cos\theta]}{\mathrm{d}E'} = \frac{(A+1)^2}{2A}\frac{1}{E} \implies \frac{\mathrm{d}P}{\mathrm{d}E'} = \frac{\mathrm{d}P}{\mathrm{d}[\cos\theta]} \cdot \frac{(A+1)^2}{2A}\frac{1}{E}.$$

- The distribution of $\cos\theta$ is found from scattering cross section via

$$\frac{\mathrm{d}P}{\mathrm{d}[\cos\theta]} = \frac{1}{\sigma_{\text{tot}}} \int \frac{\mathrm{d}\sigma}{\mathrm{d}\Omega}\,\mathrm{d}\phi,$$

where the integral runs over only azimuthal angle ϕ because θ dependence is left in the $\cos\theta$ term. In practice, the neutron scattering cross section $\frac{\mathrm{d}\sigma}{\mathrm{d}\Omega}$ is complicated; for simplicity, we will use the approximation of isotropic scattering

$$\frac{\mathrm{d}\sigma}{\mathrm{d}\Omega} = \frac{\sigma_{\text{tot}}}{4\pi},$$

in which scattering is independent of azimuthal angle. This is a good approximation for low-energy neutrons scattering from light nuclei. Assuming $\frac{\mathrm{d}\sigma}{\mathrm{d}\Omega} = \frac{\sigma_{\text{tot}}}{4\pi}$, we have

$$\frac{\mathrm{d}P}{\mathrm{d}[\cos\theta]} = \frac{1}{\sigma_{\text{tot}}} \cdot \frac{\sigma_{\text{tot}}}{4\pi} \cdot \int \mathrm{d}\phi = \frac{2\pi}{4\pi} = \frac{1}{2}.$$

The distribution of neutron post-collision energy is then

$$\frac{\mathrm{d}P}{\mathrm{d}E'} = \frac{\mathrm{d}P}{\mathrm{d}[\cos\theta]} \frac{\mathrm{d}[\cos\theta]}{\mathrm{d}E'} = \frac{1}{2} \cdot \frac{(A+1)^2}{2A} \frac{1}{E} = \frac{1}{1-\alpha} \frac{1}{E},$$

where we have used α from Equation 6.4. Finally, we recall the bounds on neutron energy from Equation 6.3 to get the complete result

$$\frac{\mathrm{d}P}{\mathrm{d}E'} = \begin{cases} 0 & E' < \alpha E \\ \frac{1}{(1-\alpha)E} & E' \in (\alpha E, E) \\ 0 & E' > E. \end{cases} \tag{6.5}$$

To summarize: this is the distribution of a fast neutron's ($E \gg k_B T$) post-collision energy E' after scattering from a single nucleus with mass number given by α via Equation 6.4. Note the result is just a uniform distribution, because of the assumption of uniform scattering.

6.2.2 Slowing Neutrons to Thermal Energy

- We will now derive an estimate for the number of collisions N required for a fast neutron with energy $E_0 = 2\,\text{MeV}$ to slow down to the thermal energy $E_{\text{T}} = 1\,\text{eV}$.
- From Equation 6.5, a fast neutron's ($E \gg k_B T$) post-collision energy E' after scattering from a single nucleus with mass number A is distributed as

$$\frac{\mathrm{d}P}{\mathrm{d}E'} = \begin{cases} 0 & E' < \alpha E \\ \frac{1}{(1-\alpha)E} & E' \in (\alpha E, E)\,, \\ 0 & E' > E \end{cases} \quad \text{where } \alpha = \frac{(A-1)^2}{(A+1)^2}.$$

We aim to find required number of collisions neutron to slow down to energy E_{T}. Principle is to first slow neutrons, then detect them.

- We first define the dimensionless parameter ξ, which encodes the average energy lost by a neutron in a single collision, according to

$$\xi \equiv \left\langle \ln \frac{E_0}{E'} \right\rangle \implies \ln \frac{E'}{E_0} = -\xi \implies E' = E_0 e^{-\xi}, \tag{6.6}$$

where we have dropped the expectation signs after the first equality for conciseness.

After one collision, a neutron's energy decreases to $E_1' = E_0 e^{-\xi}$, after the second collision to $E_2' = E_1' e^{-\xi} = E_0 e^{-2\xi}$, and so on... A neutron's energy after the N-th collision is then

$$E_N' = e^{-N\xi} E_0.$$

To find the problem's required number of collisions N to slow a neutron to thermal energy E_T, we set $E_N' \equiv E_T$ and get

$$E_\mathrm{T} = E^{-N\xi} E_0 \implies N = \frac{1}{\xi} \ln \frac{E_0}{E_\mathrm{T}}.$$

- We now return to computing ξ in Equation 6.6, which we find with the distribution of neutron post-collision energy $\frac{\mathrm{d}P}{\mathrm{d}E'}$:

$$\xi \equiv \left\langle \ln \frac{E_0}{E'} \right\rangle = \int_{E'_\mathrm{min}}^{E'_\mathrm{max}} \ln \frac{E_0}{E'} \frac{\mathrm{d}P}{\mathrm{d}E'} \,\mathrm{d}E' = \frac{1}{(1-\alpha)E_0} \int_{\alpha E_0}^{E_0} \ln \frac{E_0}{E'} \,\mathrm{d}E',$$

where we have substituted in $E'_\mathrm{min} = \alpha E_0$ and $E'_\mathrm{max} = E_0$ from Equation 6.3. We solve the integral by defining the new variable $u \equiv E'/E_0 \implies \mathrm{d}u = (\mathrm{d}E')/E_0$, which produces the expression

$$\xi = \frac{1}{1-\alpha} \int_\alpha^1 \ln u \,\mathrm{d}u = -\frac{1}{1-\alpha} \Big[u\big(\ln u - 1\big) \Big]_\alpha^1 = 1 + \frac{\alpha}{1-\alpha} \ln \alpha.$$

We then substitute in $\alpha = \left(\frac{A-1}{A+1}\right)^2$ from Equation 6.4 to get

$$\xi = 1 + \frac{(A-1)^2}{2A} \ln \frac{A-1}{A+1}.$$

For heavy nuclei with $A \gg 1$, we can simplify ξ with the Taylor expansion

$$\ln \frac{x-1}{x+1} \sim 2\left(\frac{1}{x} + \frac{1}{3x^3} + \frac{1}{x^5} + \cdots\right),$$

which produces, up to first order in A, the result

$$\xi \approx 1 - \frac{A^2 - 2A - 1}{A^2} \sim \frac{2}{A}.$$

Without derivation, a better approximation for ξ, which is exact up to one percent of the true value for $A > 10$, is

$$\xi \approx \frac{2}{A + 2/3}.$$

Remark: Neutron Absorption in Compound Materials

- For materials containing multiple elements, we generalize ξ to the average value

$$\overline{\xi} = \frac{\sum_i \sigma_i \xi_i}{\sum_i \sigma_i},$$

where σ_i is the cross section for neutron scattering in the i-th element of the absorber.

- The table below shows values the number of collisions N required to slow a single neutron of energy 2 MeV to 1 eV.

Material	A	ξ	N
Hydrogen H	1	1	15
Deuterium D	2	0.75	20
Water H_2O	-	0.5	29
Iron Fe	56	0.035	414

Lithium Silicates For Neutron Detection

- In passing, lithium silicates (essentially glass materials in everyday terms) are useful for neutron detection because: they contain enough low-A material to slow thermal neutrons and also act as scintillators.

  So lithium silicates serves as sort of "two-in-one" fast neutron detectors in that they both slow down fast neutrons and detect slow neutrons.

- Slow neutron detection interaction:

$$n + {}^6\mathrm{Li} \rightarrow {}^3\mathrm{H} + {}^4\mathrm{He}.$$

  The alpha particle ^{4}He can then be detected with standard procedures for detecting heavy charged particles.

7 Photon Detection

In this chapter we briefly outline the working principles of common photon detectors.

7.1 Photomultiplier Tubes

- A typical photomultiplier tube (PMT) is constructed from:
  (i) a photocathode electrode, held at a larger potential of the order $U_0 \sim 1\,\mathrm{kV}$,
  (ii) a series of secondary electrodes called dynodes (of the order e.g. 10), and
  (iii) a grounded anode electrode.

  The entire instrument is typically enclosed in a vacuum chamber.
- In practice, photomultiplier tubes are typically coupled to a scintillator, which emits scintillation photons in response to incident particles passing through.

  Working principle:
  (i) a scintillation photon incident on the PMT cathode frees an electron via the photoelectric effect
  (ii) the photoelectron accelerates through the dynode chain, and frees secondary electrons on each collision with a dynode
  (iii) secondary electrons free more electrons further down the dynode chain, resulting in a large number of final electrons from a single initial photoelectron
  (iv) the secondary electrons are collected at the anode, where they produce a measurable current pulse indicating the presence of the initial particle passing through the scintillator.
- If the initial scintillation photon has energy $h\nu$, the photoelectron has energy

$$T_\mathrm{e} = \hbar\nu - \Phi,$$

  where Φ is the cathode material's work function. Typical values are given below:

Material	Φ [eV]
Silver	3.4
Lithium	2.9
Platinum	5.2

- In practice, PMT cathodes do not have perfect efficiency, meaning that not every scintillation photon incident on the photocathode produces a photoelectron. The PMT's quantum efficiency is defined as

$$\eta(\lambda) = \frac{\text{number of photoelectrons}}{\text{number of incident photons}} \equiv \frac{N_\mathrm{pe}}{N_\gamma}.$$

  The quantum efficiency depends cathode material. Typical cathodes are made of semiconducting cathodes together with alkali metals (e.g. typically antimony) for a larger efficiency.

  Quoting from lecture, typical quantum efficiencies are of the order 10 to 20 percent for semiconducting/metal mixtures, but only 0.01 percent for pure metals.

- PMTs are typically useful for light in the near-infrared, visible, and ultraviolet range. Typical PMT multiplication factors for a single photoelectron are of the order 10^6 to 10^7.
- Some disadvantages of PMTs include:
  - The anode and cathode must be held at a large (kilovolt-order) potential difference
  - Poor operation in magnetic fields (which are often present in particle detectors)
  - PMTs tend to be bulky and somewhat difficult to work with mechanically.

7.2 Semiconductor Photon Detectors

7.2.1 Microchannel Plates

- Microchannel plates are disks of semiconducting material with thickness of the order $\sim 1\,\text{mm}$. Within the disk are bored small cylindrical channels with width of the order 10 to 100 µm.
- Working principle: the plate faces are held at a potential difference. A photon is incident in a channel frees a photoelectron via the photoelectric effect, and the photon is accelerated through the channel as through a dynode chain, with each collision freeing additional electrons.
- Typical microchannel plate multiplication factors are of the order $\sim 10^4$.
- Advantage: the presence of multiple channels gives precise position information—the channel outputting the strongest electrical signal indicates the position of the incident photon.

7.2.2 Avalanche Photodiodes

- Construction: from left to right in plane of paper from point of incidence to point of detection:

  (i) a thin layer of p^+ semiconductor held at negative potential

  (ii) a wide compensated layer

  (iii) a thin p-type layer

  (iv) a thin n^+ layer held at a positive potential, used as an ohmic contact.
- Like in PIN diodes, the electric field in the compensated i-type region is roughly constant, but increases considerably between the i-type and p-type regions.

  For orientation, typical electric fields in the p-type region are $E \sim 10^5\,\text{V}\,\text{cm}^{-1}$, while dielectric breakdown in silicon occurs around $E_{\text{max}} \sim 3 \cdot 10^5\,\text{V}\,\text{cm}^{-1}$. In other words, the p-type region electric field is near the regime of dielectric breakdown.
- Working principle: a photoelectron incident in i-type region is acceleration through i-type region by the constant electric field into the p-type region, where the large electric field accelerates the electron to large enough energy to free an avalanche of secondary electron-hole pairs.
- Typical multiplication factors in APDs are of the order only 10 to 100.

However, APDs have large quantum efficiency e.g. of the order 80 to 90 percent (albeit in a small wavelength range)

Hybrid Avalanche Photodiodes

- Hybrid avalanche photodiodes (HAPDs) are a variation of APDs with larger multiplication factors.
- The basic components of an HAPD are:
  1. a photocathode held at kilovolt-order negative potential
  2. an empty vacuum region
  3. a grounded APD

  The entire apparatus, like a PMT, is held in an external housing.
- Working principle:
  (i) A photon incident on the cathode frees a photoelectron via the photoelectric effect
  (ii) the photoelectron is accelerated across the potential difference in the vacuum region and strikes the APD, where it frees a large number secondary electrons.

  The potential difference between the cathode and APD is large, so the photoelectron reaches high enough energies to free of the order 10^3 secondary electrons in the APD. These secondary electrons are further multiplied in the APD itself, resulting in an HAPD multiplication factor of the order $5 \cdot 10^4$.

8 Radiation Safety

In this section we briefly outline the basic concepts and relevant physical quantities involved in the field of radiation safety, which is of course an important consideration to scientists working with ionizing radiation.

8.1 Quantities Involved in Radiation Safety

- Radioactive sources are typically divided into alpha, beta, and gamma radiation, which all have different interactions in matter and different effects on the body.

  While α, β and γ radiation are most common in everyday applications, there are of course other radiation sources, for example radiation from protons and neutrons.

- The basic physical quantity involved in radiation safety is *radioactive activity*, defined as the number of radioactive events per unit time. Radioactive activity is measured in units called becquerels; one becquerel is one event per second.

- Many radioactive sources obey an exponential decay law of the form

$$\frac{\mathrm{d}N}{\mathrm{d}t} = -\lambda N \implies N(t) = N_0 e^{-\lambda t},$$

  where N_0 is the initial number of radioactive particles and λ (units time^{-1}) is the material's decay constant. The activity of an exponentially-decaying source is simply

$$A(t) = \lambda N(t) = \lambda N_0 e^{-\lambda t}.$$

- Of course, different sources of radiation have different effects on the body; some sources are more and some less dangerous. As a result, dangerous radiation levels are quoted in the number of becquerels for a given radiation source (i.e. is not meaningful in the context of radiation safety to simply quote an activity level in becquerels without specifying the source).

  For orientation, dangerous activity levels are of the order $6 \cdot 10^{10}$ Bq for americium-241 and of the order 10^{11} Bq for cesium-137.

Absorbed Dose and Dose Rate

- Absorbed dose, denoted by D, is a physical quantity defined as the energy deposited by radiation in material per unit material mass.

  Absorbed dose is measured in units called grays; one gray is one joule per kilogram.

- Absorbed dose is commonly quoted in terms of dose rate $\frac{\mathrm{d}D}{\mathrm{d}t}$, which is simply absorbed dose per unit time.

- Note that absorbed dose and dose rate are purely physical quantities without direct biological meaning—different radiation sources with equivalent dose rates may have different effects on the human body.

Equivalent Dose

- Equivalent dose is an empirically constructed unit that attempts to correct for the fact that radiation sources producing identical dose rates may have different biological consequences.

- The equivalent dose of a given radiation source is denoted by H and defined as

$$H = \sum_i w_i D_i,$$

where the sum runs over all radiation types present in the source , (e.g. α, β, γ,etc...), and the w_i are phenomenologically-determined, dimensionless weights estimated the relative effect of each radiation type on the human body.

- For orientation, quoting from lecture, approximate values of the weights w_i for common radiation types are given below:

Radiation	w (approximately)
α	20
β	1
γ	1
p	5
n	5-20

Note that heavier particles tend to be more biologically damaging at a given absorbed dose level.

- Equivalent dose (despite have the same physical units as absorbed does D) is measured in units called sieverts to avoid ambiguity with absorbed dose.

Effective Dose

- Effective dose is a sort of generalization of equivalent dose; effective dose also includes weights for the effect of a given radiation type in different organs.

- Effective dose is denoted by E and is defined as

$$E = \sum_i k_i H_i = \sum_{i,j} k_i w_j D_j,$$

where the weights k_j are phenomenologically determined for a given organ, and the sum over j runs over relevant organs.

- For orientation, quoting from lecture, approximate values of the weights k_i for common organs are given below

Radiation	k (approximately)
Red blood marrow Large intestine Stomach	0.12
Gonads	0.08
Bladder, Gullet Liver, Thyroid	0.04
Brain, Cartilage Salivary glands, Skin	0.01

8.2 Biological Consequences

We only briefly summarize the biological consequences of radiation exposure. The consequences of radiation exposure are divided into two groups: deterministic and stochastic effects.

Deterministic Effects

- Deterministic effects are generally well-defined, occur soon (days or perhaps weeks) after initial exposure, and are relatively predictable and often deadly.
- Deterministic effects depend on absorbed (or equivalent) dose, but not effective dose.
- The damage from deterministic effects grows exponentially with absorbed dose (e.g. in grays) *above a threshold level* e.g. of roughly 2 Gy.

Stochastic Effects

- Stochastic effects are chronic and take a long time to appear (e.g. years after radiation exposure).
- In the context of stochastic effects, we speak of the probability that effects occur increasing with increasing dose, (rather than the damage from effects increasing as in deterministic effects).
- Note that stochastic effects, like deterministic effects, may also be deadly; these are typically cancer or birth defects in children.
- In passing, we note that most known information about stochastic effects is based on long-term studies of survivors of the nuclear bombings of Hiroshima and Nagasaki in World War II, and from survivors of the of the Chernobyl disaster in 1986. (And not based on data gathered from intentionally-exposed volunteers!)

Legal Limitations On Radiation Exposure

- Maximum permissible thresholds for annual radiation exposure are agreed upon by scientists and legislators are a national or international level.

  These levels must then be respected by relevant authorities responsible for occupational or residential exposure (for example, legislation in the Eastern United States requires the presence of radon filtration systems in residential housing).

- With respect to radiation exposure, the population is divided into two categories:

  (a) specialized professionals, such as particle physicists, x-ray technicians, workers in nuclear reactors, etc..., and

  (b) the general civilian population.

  Permissible dose thresholds for people in the professional category are larger by roughly an order of magnitude, and professionals are required to carry personal dosimeters in occupational settings to monitor their exposure.

- Quoting from lecture, typical permissible effective doses are of the order $10\,\mathrm{mSv\,year^{-1}}$ for professionals and $1\,\mathrm{mSv\,year^{-1}}$ for civilians.

  Typical permissible *equivalent* doses are of the order $100\,\mathrm{mSv\,year^{-1}}$ for professionals and $10\,\mathrm{mSv\,year^{-1}}$ for civilians.